

1 **Wet deposition in the remote western and central Mediterranean** 2 **as a source of trace metals to surface seawater**

3 Karine Desboeufs¹, Franck Fu¹, Matthieu Bressac^{2,3}, Antonio Tovar-Sánchez⁴, Sylvain Triquet¹,
4 Jean-François Doussin⁵, Chiara Giorio^{6,7}, Patrick Chazette⁸, Julie Disnaquet^{9,10}, Anaïs Feron¹,
5 Paola Formenti¹, Franck Maisonneuve⁵, Araceli Rodríguez-Romero⁴, Pascal Zapf⁵, François
6 Dulac⁸ and Cécile Guieu³

7 ¹ Université de Paris and Univ Paris Est Creteil, CNRS, LISA, UMR 7583, F-75013 Paris, France

8 ² Institute for Marine and Antarctic Studies, University of Tasmania, Hobart, Tasmania, Australia.

9 ³ Laboratoire d'Océanographie de Villefranche (LOV), CNRS-Sorbonne Université, INSU, Villefranche-sur-Mer,
10 06230, France.

11 ⁴ Department of Ecology and Coastal Management, Institute of Marine Sciences of Andalusia (CSIC), 11510 Puerto
12 Real, Cádiz, Spain.

13 ⁵ Univ Paris Est Creteil and Université de Paris, CNRS, LISA, UMR 7583, F-94010 Créteil, France

14 ⁶ Laboratoire de Chimie de l'Environnement (LCE), UMR 7376 CNRS, Aix-Marseille Université, Marseille, 13331,
15 France.

16 ⁷ Yusuf Hamied Department of Chemistry, University of Cambridge, Lensfield Road, CB2 1EW, Cambridge, United
17 Kingdom

18 ⁸ Laboratoire des Sciences du Climat et de l'Environnement (LSCE), UMR 8212 CEA-CNRS-UVSQ, Institut Pierre-
19 Simon Laplace, Univ. Paris-Saclay, 91191 Gif-sur-Yvette, France.

20 ⁹ Marine Biology Research Division, Scripps Institution of Oceanography, UCSD, USA

21 ¹⁰ Sorbonne Université, CNRS, Laboratoire d'Océanographie Microbienne, LOMIC, France

24 *Correspondence to:* Karine Desboeufs (karine.desboeufs@lisa.ipsl.fr)

31 **Abstract.** This study reports the only recent characterisation of two contrasted wet deposition events
32 collected during the PEACETIME cruise in the open Mediterranean ~~open-S~~seawater, and their
33 impact on trace metals (TMs) marine stocks. Rain samples were analysed for Al, 12 TMs ~~trace~~
34 ~~metals (TMs hereafter, including~~ (-Co, Cd, Cr, Cu, Fe, Mn, Mo, Ni, Pb, Ti, V and Zn) and nutrients
35 (N, P, ~~d~~Dissolved oOrganic cCarbon) concentrations. The first rain sample collected in the Ionian
36 Sea (~~R~~rain ION) was a ~~wet~~ typical regional background wet deposition event whereas the second
37 rain sample collected in the Algerian Basin (~~R~~rain FAST) was a Saharan dust wet deposition event.
38 Even in remote Med Sea, the background TM inputs presented an anthropogenic signature, except
39 for Fe, Mn and Ti. The concentrations of TMs in the two rain samples were significantly lower
40 compared to concentrations in rains collected at coastal sites reported in the literature, ~~suggesting~~
41 ~~either less anthropogenic influence in the remote Mediterranean environment, or due to the~~
42 ~~decrease~~ of anthropogenic emissions during the last-preceding decades ~~in the Mediterranean Sea~~.
43 The atmospheric TM inputs were mainly as dissolved forms even in dusty Rain FAST. The TMs
44 ~~inventories-stocks~~ in the ~~surface microlayer and~~ mixed layer (ML, 0-20_m) at ~~ION and~~ FAST
45 stations before and after the events, ~~compared to atmospheric fluxes~~, showed that the atmospheric
46 inputs were ~~a significant source~~ a significant supply of particulate TMs and of dissolved s for both
47 layers Fe and Co for surface seawater. Even if the wet deposition delivered TMs already as soluble
48 forms, the- post-deposition aerosol dissolution could to be a key additional pathway in the supply
49 of dissolved TMs. At the scale of the western and central Mediterranean, the atmospheric inputs
50 were of the same order of magnitude as ~~marine~~ML stocks ~~within the ML~~ for dissolved Fe, Co and
51 Zn, ~~underlining-highlighting~~ the role of the atmosphere in their biogeochemical cycles in the
52 stratified Mediterranean Sea. ~~In case of~~ In case of -intense dust-rich wet ~~dust~~ deposition events, the
53 role of atmospheric inputs as external source is extended, ~~the contribution of atmospheric inputs~~
54 ~~could be critical for dissolved stocks of the majority of~~ dissolved Co, Fe, Mn, Pb and Zn.TMs.
55 Our results suggest that the wet deposition constitutes only a source of some of dissolved TMs for
56 Med surface waters. The contribution of dry deposition on the atmospheric TM inputs need to be
57 investigated.

58 1. Introduction

59 Atmospheric deposition of continental aerosol has long been recognized to influence trace element
60 concentrations in remote oceanic surface waters (Buat-Ménard and Chesselet, 1979; Hardy, 1982;
61 Buat-Ménard, 1983). In particular, the Mediterranean Sea (Med Sea) is an oligotrophic environment
62 where marine ~~biosphere-microbial~~ growth is nutrient-limited during the long Mediterranean summer
63 season, which is characterized by a strong thermal stratification of surface waters (The Mermex
64 Group, 2011). The Mediterranean atmosphere is characterized by the permanent presence of
65 anthropogenic aerosols from industrial and domestic activities around the basin (e.g., Sciare et al.,
66 2003; Kanakidou et al., 2011). In addition to this anthropogenic background, the Mediterranean
67 basin is also subject to seasonal contributions of particles from biomass fires in summer (Guieu et
68 al., 2005) and to intense sporadic Saharan dust inputs (e.g., Loÿe-Pilot and Martin, 1996; Vincent
69 et al., 2016). Several studies have emphasized that the atmospheric deposition of aerosols, notably
70 through wet deposition, plays a significant role in the marine cycles of ~~both~~-nutrient, such as
71 nitrogen (N) and phosphorus (P) (e.g. Pulido-Villena et al., 2010; Richon et al., 2018 a and b;
72 Violaki et al., 2018) and micronutrients, such as iron (Fe) (Bonnet and Guieu, 2006). Recently,
73 atmospheric dust inputs were identified to have a fertilizing effect on ~~the-planktonic~~ stocks and
74 fluxes, even in the presence of relatively high dissolved nutrients N, P and Fe ~~marine~~-concentrations
75 (Ridame et al., 2011; reviewed in Guieu and Ridame, 2021). Mackey et al. (2012) showed that TMs
76 provided by dust deposition could explain this fertilizing effect. Indeed, some-many TMs, including
77 Mn, Co, Ni (Mackey et al., 2012), Cu (Annett et al., 2008) and Zn (Morel et al., 1991), play
78 physiological roles for phytoplanktonic organisms. These TMs are present in very low
79 concentrations in oligotrophic systems such as the Med Sea, possibly limiting (or co-limiting) the
80 phytoplankton growth (Pinedo-Gonzàles et al. 2015) and ~~implying-pointing to the importance the~~
81 ~~role~~-of dust deposition as source of TMs for planktonic communities. On the other hand,
82 atmospheric deposition of European aerosols ~~s-particules~~ was identified to have a negative effect on
83 chlorophyll concentrations (Gallisai et al. 2014), by providing ~~trace-metals, as~~-Cu, at toxic levels
84 (Jordi et al. 2012).

85 The atmospheric deposition of TMs in the Mediterranean is related to both dust and anthropogenic
86 aerosols deposition (Desboeufs et al., 2018). The role of dust deposition as a source of TMs was
87 observed from the correlation between the atmospheric deposition of mineral dust, and the
88 enrichment of dissolved TMs (Cd, Co, Cu, Fe) in the Medi~~terranean~~ Sea surface microlayer
89 (SML)(Tovar-Sánchez et al., 2014). For the water column, the adding of dissolved Fe and Mn was
90 emphasized in mesocosm experiments after dust addition mimicking intense wet dust deposition

(Wuttig et al., 2013). Bacconnais et al. (2019) showed that the dissolved Cu isotope signature in surface waters could be related to Saharan dust deposition in the Southern Med Sea. By comparison based on annual or monthly deposition measurements and marine concentrations, the potential role of atmospheric deposition as source of dissolved Co and Fe for Mediterranean surface waters was also pointed (Bonnet and Guieu, 2006, Dulaquais et al., 2017). Due to Mediterranean sporadic and intense storms, the rain events by scavenging loaded air masses with anthropogenic aerosols or Saharan dust could lead to higher deposition TM fluxes than dry deposition (Desboeufs et al., 2021). Moreover, even if annual wet and dry deposition are equivalent in Mediterranean (Theodosi et al., 2010), wet deposition is known to provide soluble, and potentially bioavailable forms of TMs (Jickells et al., 2016). Yet, ~~Yet, to the best of our knowledge,~~ the direct impact of wet deposition events on TMs concentrations in surface seawater has ~~never-not~~ been studied ~~-in situ, in a same location by concurrently collecting both rainwater and seawater samples before this work,~~ whether in the ~~Mediterranean-Med Sea~~ or in other oceanic regions.

~~Moreover, the t~~Two key criteria used to assess the potential impact of TMs~~ss~~ and nutrients~~ss-wet deposition are~~ are their respective concentrations (or fluxes) and fractional solubility (solubility hereafter), i.e., the partitioning between dissolved and total concentrations in rainwaters. Indeed, it is considered that the dissolved fraction of nutrients and TMs is a surrogate for their bioavailability can be directly assimilated by the phytoplankton(Jickells et al., 2016). Few studies ~~focussed on~~have reported concentrations of TMs in rainwater samples ~~was~~ collected around the Mediterranean basin: Al-Momani et al., (1998), Kanellopoulou, (2001) and Özsoy and Örnektekin, (2009) in the eastern basin, and Losno (1989), Guieu et al. (1997), Frau et al., (1996), Chester et al., (1997) and Guerzoni et al. (1999b) in the western basin. These studies led to highly variable TMs concentrations and solubilities~~y~~, illustrating ~~a more general~~the large variability of TMs inputs during wet deposition events in the ~~Mediterranean~~ Sea (reviewed in Desboeufs, 2021). All these studies were performed at coastal sites. Offshore samples of rainwater have rarely been ~~studied-reported~~ in the literature ~~so far~~. In the Mediterranean, to our knowledge, trace element concentrations from only three rain samples collected at sea in April 1981 have been reported in a PhD thesis (Dulac, 1986). However, due to the continental and local sources of pollution, ~~n-and~~ the variety of anthropogenic aerosol sources (Amato et al., 2016) and the physico-chemical processes during atmospheric aerosol transport (chemical ageing, dispersion, gravitational settling, in-cloud reactivity..)(Weinzierl et al., 2017), the TMs rain composition of the coastal zone ~~could-may~~ not be representative of atmospheric deposition ~~in-to~~ the remote Mediterranean.

The PEACETIME cruise (ProcEss studies at the Air-sEa Interface after dust deposition in the Mediterranean Sea) performed in spring 2017 aimed ~~at to~~ studying the impacts of atmospheric deposition, in particular Saharan dust events, on the physical, chemical and biological processes in this marine oligotrophic environment (Guieu et al., 2020). We investigated ~~here~~ the concentration and solubility of TMs and nutrients ~~of from~~ two rainwaters-rain events sampled in the central and western —Mediterranean open—Ssea during the cruise. We compared our results on TMs concentrations and solubility in rainwater with the existing literature on TM concentrations in offshore and coastal rain samples dating of 1990's previous studies based on rainwater samples collected at coastal sites to investigate the time evolution of TM concentrations and the potential differences with the open sea. Additionally, to assess the impact of wet deposition on the surface TMs concentrations, surface seawater ~~including the surface micro layer and rain water was were~~ concurrently collected ~~for the first time with rain samples~~. This is the first time TM data for these atmospheric and marine compartments in Med Sea have all been discussed at the same time and in a same place.

2. Sampling and methods

2.1 Sampling and chemical analysis of rainwater

The PEACETIME oceanographic campaign (<https://doi.org/10.17600/17000300>) took place in the western and central ~~Mediterranean~~ Sea on-board the French ~~research vessel~~ (R/V) *Pourquoi Pas ?* between 11 May and 10 June 2017, i.e. at the beginning of the Mediterranean stratification season (Guieu et al., 2020). The rain collector was installed on the upper deck (22 m above sea level) where no on-board activities were taking place to avoid contamination. ~~A-The~~ The rain collector was equipped with an on-line filtration system to ~~directly~~ separate the dissolved and particulate fractions at the time of collection (details of the filtration system are available in Heimburger et al., 2012) allowing for the calculation of solubility of TMs in the rainwater ~~at the time of collection~~. The filtration device was equipped with a Nuclepore® polycarbonate membrane (~~PC~~)-filter (porosity: 0.2 µm, diameter: 47 mm) ~~and the~~ and the diameter of the funnel of the collector was 24 cm. The rain collectors ~~were was~~ installed only when rain was expected and ~~kept closed within~~ covered by an acid-washed sealed plastic film ~~until the rainfall began~~ when not in use. All the sampling materials were thoroughly acid-washed in the laboratory prior to the cruise departure (washing protocol

described in Heimburger et al., 2012). No stabilizing ~~setup-device~~ was used to keep the funnel level during the pitch and roll of the ship, preventing a precise assessment of the height of rainfall from the collected water volume. During the rain sampling, the ~~ship-R/V~~ was always facing the wind to avoid contamination by the ~~smoke-of-the-ship's exhaust-itself~~, as the chimney was situated on the lower deck and behind the collector.

Immediately after sampling, the collector was disassembled under ~~the-a~~ laminar flow hood inside ~~an clean-room~~ on-board clean-room laboratory. The dissolved fraction was separated into ~~four-4~~ aliquots dedicated to ~~i)-dissolved organic carbon (DOC) by high-temperature catalytic oxidation (HTCO) on a Shimadzu total organic carbon analyzer (as described in Van Wambeke et al 2021);~~ ~~ii)-major ions by ion chromatography (IC);~~ ~~iii) TMmetals analysis determination~~ by inductively coupled plasma coupled methods (ICP), ~~ii) major ion analysis by ion chromatography (IC);~~ ~~iii) dissolved organic carbon (DOC) determination by high-temperature catalytic oxidation (HTCO) on a Shimadzu total organic carbon analyzer (as described in van Wambeke et al., 2021a);~~ and iv) pH measurement. For ICP measurements, the sample was acidified immediately to 1% by volume of ultra-pure nitric acid (\approx 67-69%, Ultrapur, Normatom®, VWR). For IC analysis, the ~~sample-filtrate~~ was immediately frozen. For DOC analysis, the filtrate was collected into pre-combusted glass ampoule and acidified to pH 2 with phosphoric acid. Ampoule was immediately sealed and stored in the dark at room temperature.

The filter (particulate fraction) was dried under the laminar flow hood, and then put in a storage box and packed with a plastic bag to avoid contamination. After returning to the laboratory, filters were acid digested by using the ~~adapted~~ protocol adapted from Heimburger et al. (2012) as follows: filters were placed in tightly capped Savillex™ PFA digestion vessels with 4 mL of a mixture of HNO₃ (67-69%, Ultrapur, Normatom®, VWR), H₂O and HF acids (40%, Ultrapur, Normatom®, VWR) in a proportion ~~(of 3: 1: 0.5)~~, then heated in an oven at 130°C for 14 hours. After cooling, ~~the~~ solution was completely evaporated on a heater plate (ANALAB, 250, A4) at 140°C for about 2h, then 0.5 mL of H₂O₂ (30-32%, Romil-UpA™) and 1 mL of the acidified water (2% HNO₃) was added to the vessels and heated during-for 30 min. to dissolve the dry residue in the bottom of the vessels; finally, 12 mL of acidified water (1% HNO₃) was added to obtain 13.5 mL of solution in a tube for ICP-~~MS~~ analyses.

The dissolved fractions and the solutions issued of digestion of the particulate fractions were analysed by ICP-AES (Inductively Coupled Plasma Atomic Emission Spectrometry, Spectro ARCOS Ametek®, Desboeufs et al., 2014) for major elements (Al, Ca, K, Mg, Na, S) and by HR-

ICP-MS (High Resolution Inductively Coupled Plasma Mass Spectrometry, Neptune Plus TM at Thermo Scientific TM) for P and TMs: Cd, Co, Cr, Cu, Fe, Mn, Mo, Ni, Pb, Ti, V and Zn. The dissolved fraction was analysed by IC (IC 850 Metrohm) for the inorganic and organic anions (NO₂⁻, NO₃⁻, PO₄³⁻, SO₄²⁻, F⁻, Cl⁻, Br⁻, HCOO⁻, CH₃COO⁻, C₂H₅COO⁻, MSA, C₂O₄²⁻) and for the cation NH₄⁺ (Mallet et al., 2017). Only TMs, major nutrients, i.e. N and P species, and Al are discussed in this manuscript. ~~On the other hand, the dissolved fraction and solution from digestion of particulate fractions were analysed by ICP-AES (Inductively Coupled Plasma Atomic Emission Spectrometry, Spectro-ARCOS Ametek®) for major elements (Al, Ca, K, Mg, Na, S) (Desboeufs et al., 2014) and by HR-ICP-MS (High Resolution Inductively Coupled Plasma Mass Spectrometry, Neptune Plus TM at Thermo Scientific TM) for TMs: Cd, Co, Cr, Cu, Fe, Mn, Mo, Ni, P, Pb, Ti, V and Zn.~~ The speciation of dissolved P was estimated by determining ~~the~~ dissolved inorganic phosphorus (DIP) from phosphate concentrations expressed as P and the dissolved organic phosphorus (DOP) from the difference between total dissolved phosphorus (TDP), obtained by HR-ICP-MS, and DIP, obtained by IC. The dissolved inorganic nitrogen (DIN) were defined as sum of NO₂⁻, NO₃⁻ and NH₄⁺, expressed as N.

In order to estimate the contamination of sampling and analytical protocols, ~~3-three~~ blanks of rain samples, ~~(collected on-board during the cruise-with the same protocol, without rain events)~~ were used and processed. Blank samples were prepared by rinsing the funnel with 150 mL of ultrapure water (18.2 mΩ cm) with the same protocol of rain collection. The procedural limit of detections (LoD) were defined as 3 x standard deviation of blank samples both for dissolved and particulate fractions estimated after acid digestion. All ~~samples~~ dissolved and particulate sample concentrations were higher than LoD, except for NO₂⁻ in the two rain samples. The blank concentrations represented 10.2% ~~in-on~~ average for TMs and were typically lower than 20% of the sample concentrations, except for Cd (52%) and Mo (43%) in the dissolved fraction. ~~For the sample concentration computations, we subtracted these blanks values to elemental concentrations obtained in rain samples~~ Blank concentrations were subtracted from all sample concentrations.

2.2 Atmospheric ancillary measurements

The PEGASUS (Portable Gas and Aerosol Sampling UnitS, www.pegasus.cnrs.fr) mobile platform of LISA is a self-contained facility based on two standard 20-feet containers, adapted with air-conditioning, rectified power, air intake and exhausts for sampling and online measurements of

218 atmospheric aerosols and gaseous compounds, and their analysis (Formenti et al., 2019). During the
219 PEACETIME cruise, only the sampling module of the facility was deployed on the starboard side
220 of deck 7 of the R/V. The PEGASUS instrumental payload of relevance to this paper included
221 measurements of the major gases such as NO_x, SO₂, O₃ and CO by online analysers (Horiba APNA,
222 APSA, APOA and PICARRO respectively; 2-min resolution, for all gases was detection limit 0.5
223 ppb and 1 ppb for CO). ~~These gases, that~~ were used to estimate the origins of ~~collected-sampled~~ air
224 ~~masses~~.

225 From the first of June 2017 (not operational before), additional measurements by an ALS450®
226 Rayleigh-Mie lidar (Leosphere™; ~~–~~Royer et al., 2011) ~~w~~aeres used to monitor the vertical
227 distribution of aerosols over time and the associated integrated columns. The vertical lidar profiles
228 were analysed to yield the apparent backscatter coefficient (ABC) corrected from the molecular
229 transmission, as well as the volume depolarisation ratio (VDR). The inversion procedure (Chazette
230 et al., 2016 and; 2019) to retrieve the aerosol extinction coefficient (unit km⁻¹) ~~used~~s a vertical-
231 dependent lidar ratio that takes~~ook~~ into account two aerosol layers. The first layer corresponded
232 marine aerosols in the marine boundary layer (MBL), the second to a desert aerosol layer that ~~can~~
233 could extend between ~1 and 6 km above mean sea level (amsl). In accordance with Chazette et al.
234 (2016), for the same wavelength and region, the lidar ratios were set to 25 and 55 sr, respectively.
235 The vertical profile of the aerosol extinction coefficient was retrieved from 0.2 km amsl ~~on-upwards~~
236 with a vertical resolution of 15 m. Based on these profiles, the integrated column content of dust
237 aerosols was estimated using a specific extinction cross-section of 1.1 m² g⁻¹ as proposed by Raut
238 and Chazette (2009).

239 In addition, detailed meteorological data such as air and sea temperature, atmospheric pressure,
240 relative humidity, atmospheric pressure, heat flux and wind speed and direction were provided on
241 a 30 seconds ~~time~~-step basis by the ship's permanent instrumentation.

242 **2.3 Sampling and analysis of dissolved TMs in seawater**

243 ~~Before and after each rain, seawater samples were collected in the surface microlayer (SML: <1~~
244 ~~mm) and subsurface seawater (SSW: <1-m depth) (Tovar-Sánchez et al., 2020, this special issue).~~
245 ~~SML and SSW samples were collected from a pneumatic boat 0.5–1 nautical mile away from the~~
246 ~~R/V in order to avoid any potential contamination. SML samples were collected using a glass plate~~
247 ~~sampler (Stortini et al., 2012; Tovar-Sánchez et al., 2019) which had previously been cleaned with~~
248 ~~acid overnight and rinsed thoroughly with ultrapure water (MQ-water). The 39 x 25-cm silicate~~
249 ~~glass plate had an effective sampling surface area of 1950-cm² considering both sides. In order to~~
250 ~~check for procedural contamination, SML blanks were collected at some stations on board of the~~

pneumatic boat by rinsing the glass plate with ultra-pure water and collecting 0.5 L of ultra-pure water using the glass plate system. The surface microlayer thickness was calculated following the formula of Wurl (2009). SSW was collected by using an acid-washed Teflon tubing connected to a peristaltic pump. The total fraction (i.e. T-SML) was directly collected from the glass plate system without filtration in a 0.5 L acid-cleaned LDPE bottles, while the dissolved fraction in the SML (i.e. D-SML) and SSW (i.e. D-SSW) was filtered *in situ* through an acid-cleaned polypropylene cartridge filter (0.22 µm; MSI, Calyx®).

TMs samples were also collected in the water column using ~~a titanium~~ the trace metals clean (TMC) rosette (mounted with 24 teflon-coated Go-Flo bottles) before and after the rain events (Bressac et al., 2021). Although rosette deployments were performed over the whole water column, we focus here on the 0-20 m marine mixed-layer (ML). ~~The water column was sampled using the TMC titanium rosette mounted with 24 teflon-coated Go-Flo bottles.~~ Immediately after recovery, the Go-Flo bottles were transferred inside a class-100 clean laboratory container. Seawater samples were directly filtered from the bottles through acid-cleaned 0.2-µm capsule filters (Sartorius Sartobran-P-capsule 0.45/0.2-µm). All samples were acidified on-board to pH < 2 with Ultrapure-grade HCl under a class-100 HEPA laminar flow hood. Metals (namely Cd, Co, Cu, Ni, Mo, V, Zn and Pb) were pre-concentrated using an organic extraction method (Bruland et al., 1979) and quantified by ICP-MS (Perkin Elmer ELAN DRC-e) in the home laboratory. ~~In order to breakdown metal-organic complexes and remove organic matter (Achterberg et al., 2001; Milne et al., 2010), total fraction samples (i.e. T-SML) were digested prior to the pre-concentration using a UV system consisting of one UV (80 W) mercury lamp that irradiated the samples (contained in quartz bottles) during 30 min.~~ The accuracy of the pre-concentration method and analysis for TMs was established using Seawater Reference Material (CASS 6, NRC-CNRC) with recoveries ranging from 89% for Mo to 108% for Pb. Due to the complexity of the analytical method, all the TMC samplings were not analysed for Cd, Co, Cu, Ni, Mo, V, Zn and Pb ~~these metals~~. Overall, 1 or 2 depths were obtained in the mixed layer (0-20 m). Dissolved Fe and Al concentrations were also measured on-board. Dissolved Fe concentrations were measured using an automated Flow Injection Analysis (FIA) with online preconcentration and chemiluminescence detection (Bonnet and Guieu, 2006), and dissolved Al concentrations using the fluorometric method described by Hydes and Liss (1976). Sampling and analysis for dissolved Fe and Al concentrations are fully described in Bressac et al. (2021), and covered at least 4-four depths in the 0-20 m mixed layer.

2.4 Concurrent sampling strategy

Our sampling strategy of collecting seawater before and after rains were, to the best of knowledge, the first direct observations intended to trace the fate of atmospheric TMs and nutrients in the water column after wet deposition events in an open ocean setting. The sampling time-resolution was optimized to obtain results before and after rains, however this strategy was very dependent on meteorological conditions. The time chart of the sampling of rain and surface water is presented in Fig. 1.

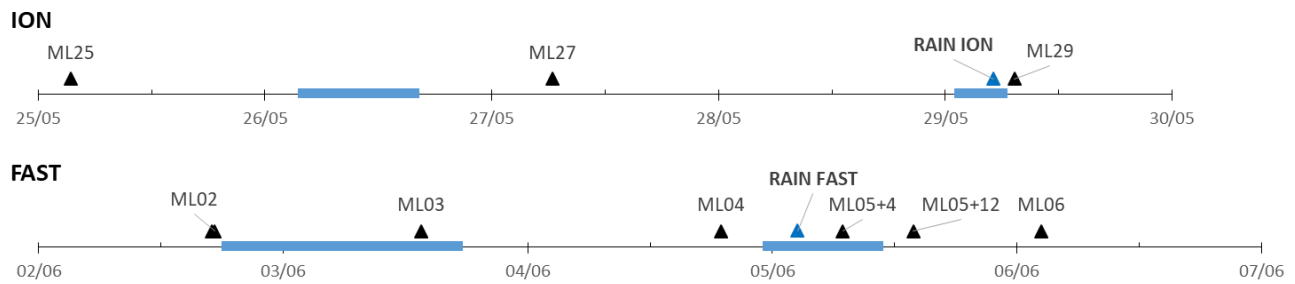


Figure 1: Sampling chronology during the ION and FAST stations for ML and rains. The blue periods correspond to rainfall in the vicinity of the R/V position (from ERA 5 reanalysis and radar imagery, see section 3.1.), and blue triangles to the rainfall on the R/V position. Samplings were performed 4 days (ML25) and 2 days (ML27) before and 2 h (ML29) after Rain ION, and at a higher frequency at the FAST station: 57 (ML02), 37 (ML03) and 7.5 (ML04) hours before and 4.5 (ML05+4), 12 (ML05+12), 24 hours (ML06) after Rain FAST.

The potential enrichment of the ML from the Rain FAST was estimated by comparing atmospheric wet deposition fluxes and marine stocks in particulate and dissolved fraction and by calculating the difference (delta) in TM stocks before and after rain. Dust rain deposition over the FAST station area started on 3 June (see section 3.1). Bressac et al. (2021) showed that the dust signature, traced by changes in Al and Fe particulate stocks in the ML, was already visible from the ML03 sampling, but not for dissolved stocks. However, they presumed also that the water mass sampled before deposition (ML02) was different from the one sampled during the rest of the time-series (ML03 to ML06) but was representative of particulate background level. In consequence, we defined the enrichment of seawater layers as the difference between the stocks after rains (ML05+4) and the initial seawater stocks (ML02 for particulate stocks (before dust signature) and ML04 for dissolved stocks (the closest sampling before the rain)).

2.4.5 Enrichment factor and solubility

In order to better constrain the origin of TMs in the rain samples, their enrichment factors (EF; Rahn 1976) relative to the Earth's crust ~~was-were~~ calculated based on their total concentrations (dissolved + particulate fractions) as:

$$EF = \frac{([X]/[Al])_{sample}}{([X]/[Al])_{crust}} \quad (1)$$

where $[X]/[Al]$ is the ratio between an element X and Al concentrations in rainwater samples (at the numerator), and in the Earth's upper continental crust (denominator) from Rudnick and Gao (2003). Aluminium is currently used as a reference element as it ~~only-predominantly~~ has a crustal origin. For a given TM, $EF > 1$ indicates an enrichment with respect to the average composition of the Earth's crust. To account for the soil composition variability of mineral dust ~~atmospheric~~ sources, TMs with an EF value > 10 are considered significantly enriched, which points to derived from non-crustal sources (Rahn, 1976). For most metals, enrichment shows important input from anthropogenic sources, due to their low content in other non-crustal sources such as seaspray or biogenic aerosols (Jickells et al., 2016).

The ~~relative-fractional~~ solubility of TMs in the two rainwater events was calculated as:

$$S_X\% = \frac{[X]_{dissolved}}{[X]_{total}} \times 100 \quad (2)$$

where $S_X\%$ is the ~~relative~~-solubility (in %) of an element X in the rainwater, $[X]_{dissolved}$ and $[X]_{total}$ are its soluble and total concentration, respectively.

2.5.6 Atmospheric wet deposition fluxes

Impacts on biogeochemical cycles and ecosystem functioning after a rain event occur on time scales of a few days (2-3), and space scales of tens of km (about 20-50 km within the radius of the ~~ship's~~ R/V position). In the specific context of oceanographic cruising, the documentation of these impacts is restricted to the vertical dimension at the prescribed temporal scale. In this vertical dimension, the exchange of TMs ~~aeross-into~~ the ML was controlled both by atmospheric inputs over the R/V position and by advection from surrounding water masses that may have been impacted by surrounding rainfall. Therefore, we had to consider this process in our estimation of the atmospheric fluxes contributions. For this purpose, the atmospheric fluxes have to be integrated to the extent of the rain area that can impact the marine surface layers. We derived wet deposition fluxes by considering the total precipitation accumulated during the duration of the rain over the area around the R/V ~~location~~position (in a radius of ~25km). Thus, the wet deposition fluxes ~~in our rain samples~~ were calculated by multiplying the ~~volume-weighted mean rainfall~~TM concentrations ($\mu\text{g L}^{-1}$ or $\mu\text{mol L}^{-1}$) in our rain samples by the total precipitation (mm) in this area. The total precipitation of

the rain events was issued from the hourly total precipitation accumulated during the rain events over the region from ERA5 ECMWF reanalysis (Herbasch et al., 2018) and from the rain rate composite radar products from the European OPERA database (Saltikoff et al., 2019), when it was possible. Although subject to uncertainties (Morin et al., 2003), a surface-based weather radar is probably the best tool to estimate rainfall in the surroundings of the R/V since this method is a direct measurement of precipitation with both a best time and spatial resolution in comparison of model estimations. However, the OPERA database does not include Italian radars, which ~~anyway~~ did not cover the central area of the Ionian Sea during the cruise anyway. ERA5 data ~~are~~ were available on regular latitude-longitude grids at 0.25° x 0.25° resolution. The accumulated precipitation was taken from the grid-points spanning the ~~ship's R/V~~ location, ~~more or less~~ ± 0.25° around the central grid-point for integrating the regional variability. Surface rain rate radar composite images were available every 15 minutes with a spatial resolution of 2 km x 2 km. The accumulated precipitation was the sum of ~~integral~~ integrated rain rates during the rain duration averaged over the radar pixels spanning the ~~ship R/V~~ location within a radius of about 25 km around ~~the ship location~~.

2.6.7 Stocks in the surface seawater

~~For the surface microlayer (SML), stocks of TMs were estimated from the integration of TMs concentration over the thickness of the layer. The thickness ranged from 32 to 43 µm and from 26 to 43 µm at ION and FAST, respectively (Tovar-Sanchez et al., 2020).~~

The trace metals stocks within the ML were calculated by trapezoidal integrations of marine concentrations from ~~SSW and~~ TMC rosette samplings. The upper water column was stratified along the cruise transect (Taillandier et al., 2020), with a ML depth (MLD) ranging from 7 to 21 m (11 to 21 m at ION station and 11 to 19 m at FAST station (Van Wambeke et al., 2020)). The ~~ML depth~~ (MLD) fluctuations, for example due to wind peaks associated with rain events, could create rapidly changing conditions of vertical advection from deeper waters. However, with no significant increase in TMs concentrations being observed below the ML down to about 50 m (not shown), the enrichment observed in the ML after rainfalls could not be attributed to any mixing with deeper water due to high wind. ~~In consequence, stocks in the ML have been integrated over a constant depth range of 0-20 m for comparison, as in accordance with~~ Bressac et al. (2021). For Cu, Fe, Ni ~~and~~ Zn, stocks were estimated both ~~for~~ for the dissolved and particulate fractions in the ~~SML and~~ ML, for Co, Cd, Mo, Pb and V only for the dissolved fraction ~~only in the ML (particulate fraction was not analysed) and for both fractions in the SML~~ and for Mn and Ti only for the particulate

fraction~~in the ML~~. The particulate and dissolved fractions of TM stock or fluxes will be mentioned as pTM and dTM respectively.

The partitioning coefficient between the particulate and dissolved phases ($K_d = [\text{particulate}]/[\text{dissolved}]$) was used to investigate exchanges between the dissolved and particulate pools of TMs.

3. Results

3.1 General conditions

The general meteorological conditions during the cruise indicated that the ION and FAST stations were highly affected by cloudy weather conditions. During these periods, 2-two significant rain events occurred overn the R/V position and ~~have been collected~~were sampled: The first samplerain (~~hereafter~~ Rain ION) was collected during the 4-day ION station occupation in the Ionian Sea in the early morning of 29/05/17 at 03:08 UTC, ~~and~~ The second rain event (~~hereafter~~ Rain FAST) occurred during the 5-day "Fast action" station occupation, (~~hereafter~~ 'FAST') in the Algerian Basin during the night of 05/06/17 at 00:36 UTC (Table 1). The two rain sample collections coincided with peaks in relative humidity and wind speed, and minima in air temperature (not shown).

Table 1: Information regarding the two rains collected during the PEACETIME cruise.

Sample	Sampling time	Station name (dates) and rain location	Estimated total precipitation
Rain ION	29 May 2017, 03:08-04:00 (UTC) 05:08-06:00 (local time)	ION (25-29 May) 35.36°N, 19.92°E	3.5 ± 1.2 mm
Rain FAST	05 June 2017, 00:36-01:04 (UTC) 02:36-03:04 (local time)	FAST (2-7 June) 37.94°N, 2.91°E	6.0 ± 1.5 mm

3.1.1. Rain ION

The ERA 5 data reanalysis shows 2-two periods of precipitation in the surrounding vicinity of the ship's R/V position, i.e. in the morning and evening of 26 June ~~26~~ (not shown) and in the night between ~~June~~ 28 and 29 June 2017, in agreement with on-board visual observations. The rain event

394 collected at ION was the product of a large cloud system, covering an area of about 90 000 km²
 395 around the R/V position, spreading over the Ionian and Aegean Seas (Fig. 24). ~~As no~~ radar
 396 measurements ~~being were~~ available for this area, the accumulated ~~precipitation rate~~ (3.5 ± 1.2 mm)
 397 was estimated from ERA 5 data reanalysis on the grid-point corresponding to the ION station
 398 (~~±0.25°~~) ~~and was 3.5 ± 1.2 mm~~ around the R/V position (~~±0.25°~~). The wash-out of the atmospheric
 399 particles was revealed by the decrease in aerosol number concentrations monitored on-board from
 400 about 1900 to 300 part.cm⁻³ (supplementary material Fig. S1). Air mass back-trajectories showed
 401 that the scavenged air masses came from Greece both in the marine boundary layer and in the free
 402 troposphere (Fig. S1). The satellite observations ~~also~~ showed low aerosol optical thickness during
 403 this period (not shown), meaning low amounts of aerosols in the atmospheric column. No significant
 404 European pollution influence was monitored by ~~on-~~board measurements during this event, with
 405 major gas mixing ratios and aerosol concentrations ~~in close to~~ the average values of the cruise (Fig.
 406 S1) ~~and typical of clean atmospheric concentrations,~~ i.e. under ~~detection~~ limit ~~of detection~~ for
 407 NO_x, 1.2 ppb for SO₂, 51 ppb for O₃, 80 ppb for CO and 3000 part.cm⁻³. On this basis, this wet
 408 event was representative of a Mediterranean background marine rain event.

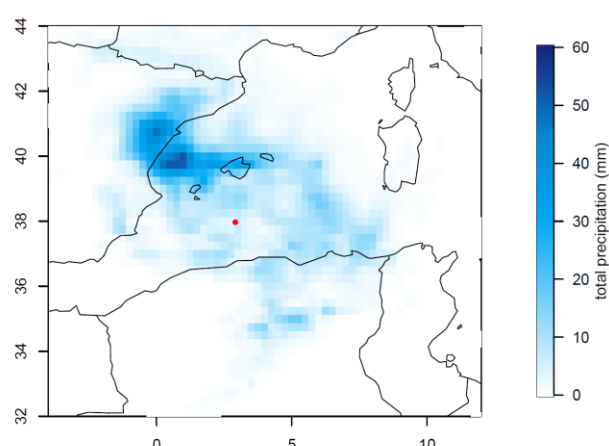
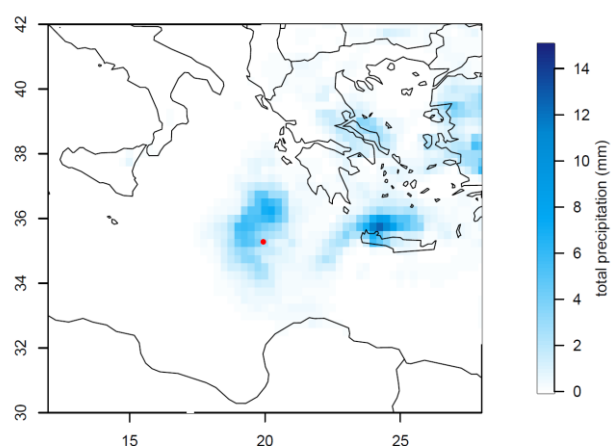
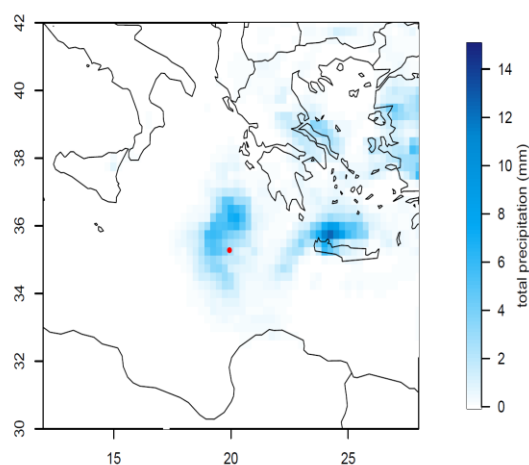
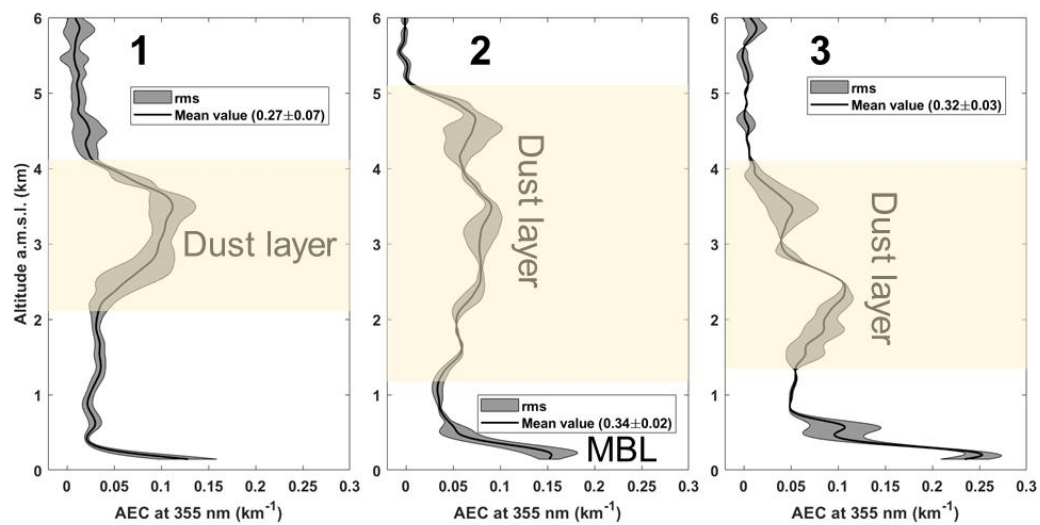
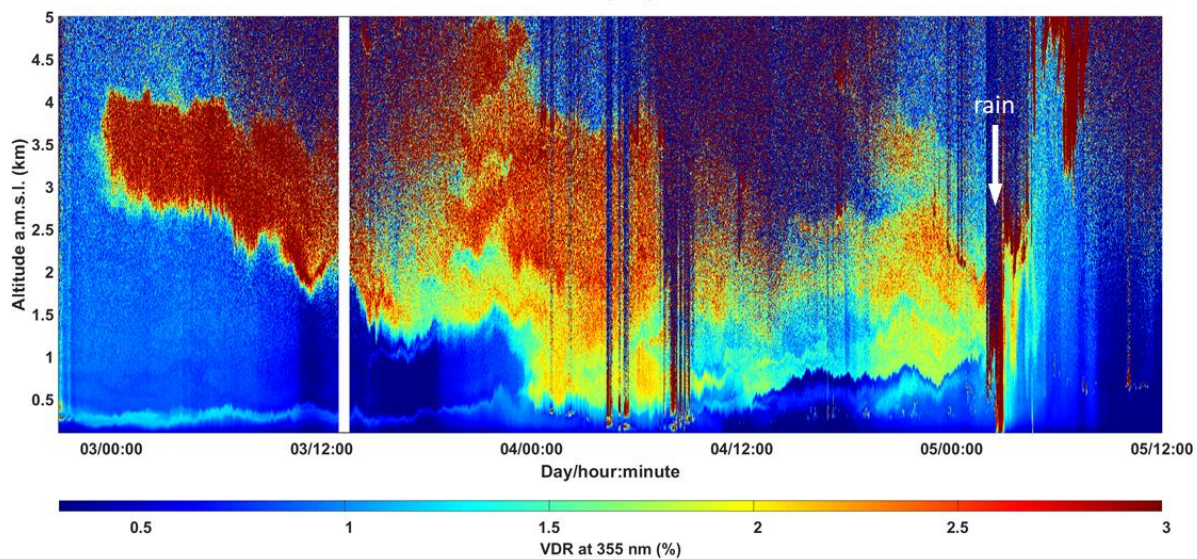
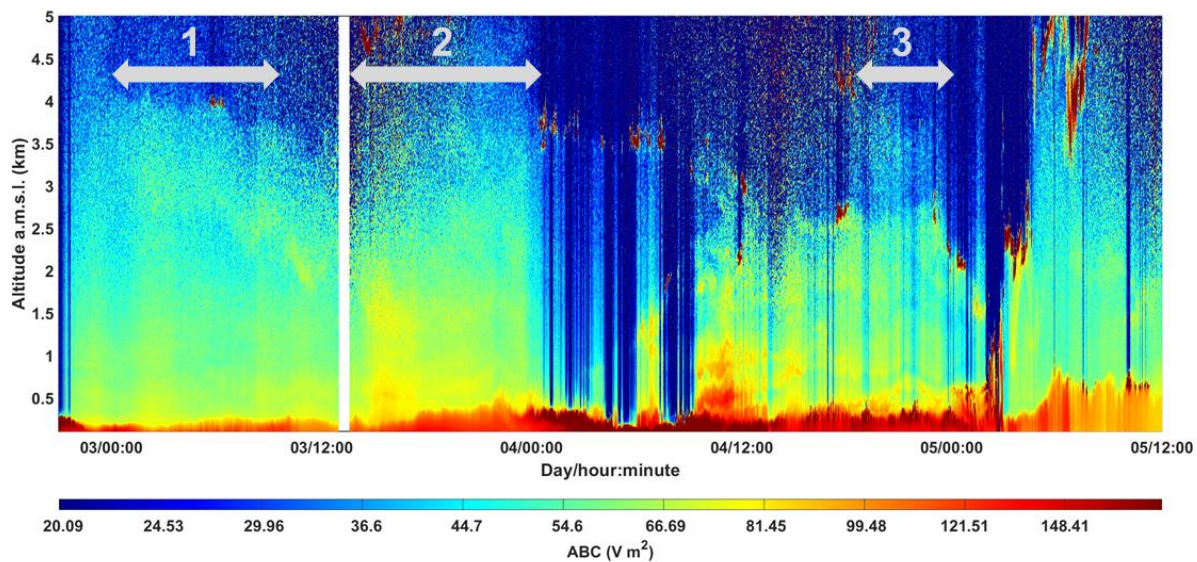


Figure 12: Total precipitation (mm) between ~~May-28~~ May at 20:00 UTC and 29 May 2017 at 10:00 UTC (Rain ION, left figure) and between the 4 June at 20:00 and 5 June 2017 at 09:00 UTC (Rain FAST right figure) from ERA5 ECMWF reanalysis. The red circle indicates the R/V position. Note different scales for total precipitation.

3.1.2. Rain FAST

As detailed in Guieu et al. (2020), the FAST station position was decided on the basis of regional model forecast runs and satellite observations, ~~in-for~~ the purpose ~~to-of~~ catching a wet dust deposition event. Significant dust emissions were observed from NASCube (<http://nascube.univ-lille1.fr/>, Gonzales and Briottet, 2017) over North Africa from the night of 30-31 May 2017, then new dust emissions in the night from 3 to 4 June 2017 in Algeria and southern Morocco associated with a northward atmospheric flux. On 30 May, the SEVIRI AOD satellite product (<https://www.icare.univ-lille.fr/data-access/browse-images/geostationary-satellites/>, Thieuleux et al., 2005) confirmed the presence of atmospheric dust in a cloudy air mass over the western part of the Mediterranean, and from 2 June -the export of a dust plume from North Africa south of the Balearic Islands with high AOD (>0.8) on the Alboran Sea was observed (Fig. S2). The dust plume was transported to the NE up to Sardinia on ~~June-4~~ June, with AOD <0.5 ~~in all the area and~~ ~~e~~Clear sky with low AOD was left west of 4°E on ~~June-5~~ June.

On-board lidar measurements (Fig. 2-3 a,b,c) showed that the aerosol plume was present over the ~~ship-R/V~~ position from 2 June 2017 at 21:00 UTC until the rain event, and corresponded to a dust aerosol layer ~~well~~ highlighted by the high depolarization. The dust plume was concentrated between 3 and 4 km at the beginning of the station occupation, then expanded down to the marine boundary layer (about 500 m amsl) ~~to-by~~ the end of the day on ~~3 June 2017~~ ~~down to the marine boundary layer (about 500 m amsl)~~. The mass integrated ~~contents-concentrations~~ of dust aerosols derived from the profiles of aerosol extinction ranged from a minimum of $0.18 \pm 0.005 \text{ g m}^{-2}$ just before the rain to a maximum of $0.24 \pm 0.009 \text{ g m}^{-2}$, where standard deviations indicate the temporal variability (1 sigma).



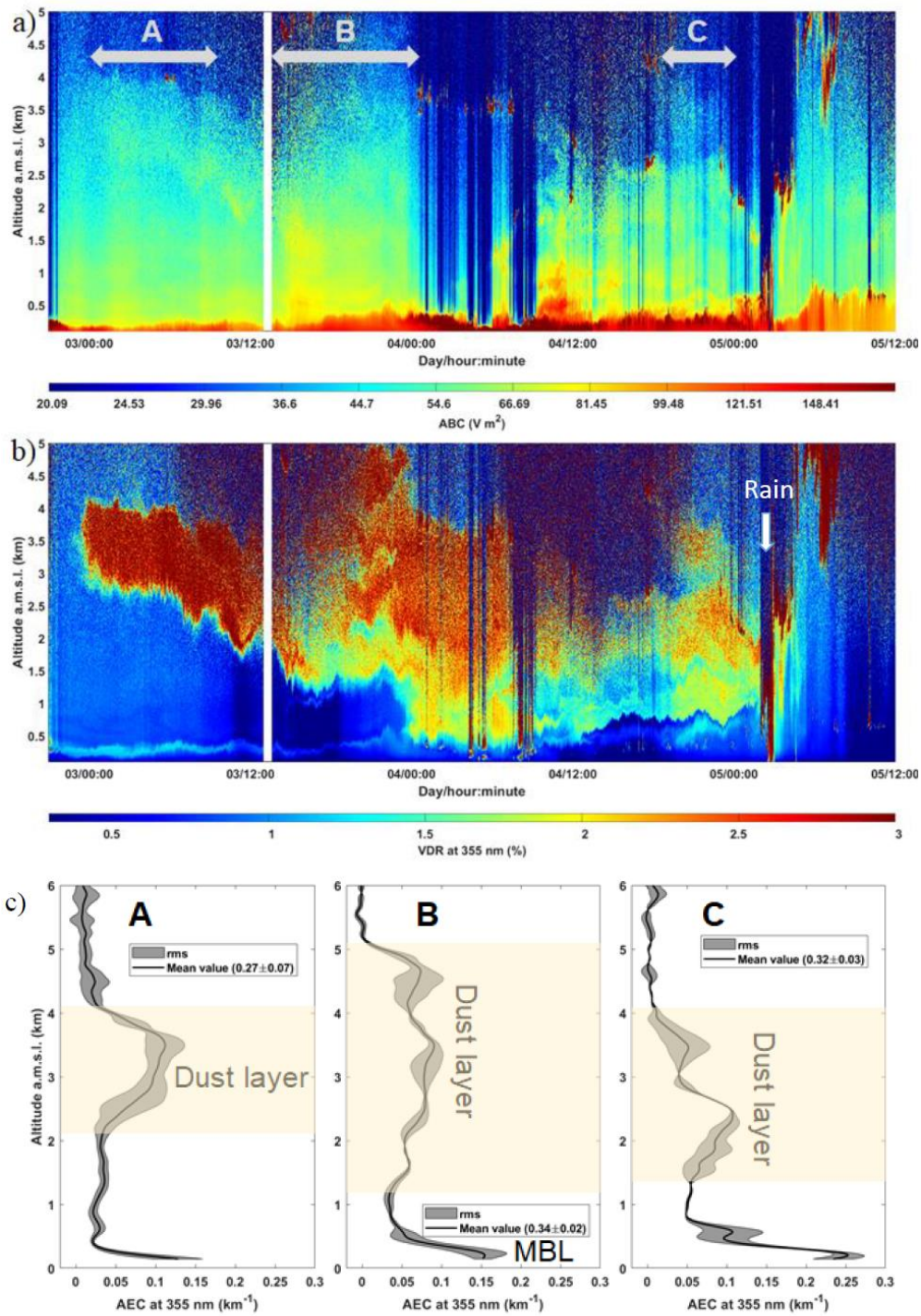


Figure 23: On-board lidar-derived: a) Apparent backscatter coefficient (ABC) (top panel), (b) Temporal evolution (in Local Time) of the lidar-derived volume depolarization ratio (VDR) (middle panel in local time) where the dust plume is highlighted for values higher than ~ 1.7 (yellow to red colours) and the rain by values higher than 3 (indicated by the white arrow), and c) vertical profiles of the aerosol extinction coefficient (AEC) in cloud free condition, integrated over 3 periods, noted 1, 2 and 3 on the top panel, along the dust plume event, noted A, B and C in figure a (bottom panels). The grey shade represents the root mean square (rms) variability along the time of the measurement.

447 The dust layer is highlighted on the profiles. The mean aerosol optical thickness is given in the boxed
448 legend with its temporal variability (1 sigma). The location of the marine boundary layer (MBL) is
449 also pointed.

450 Rainfalls ~~were~~as observed by weather radar images in the ~~neighbouring~~-area of the R/V
451 neighbouring from 3 June at 7:00 UTC. The rainfalls recorded around FAST station ~~were~~was
452 associated with 2-two periods of rain: ~~the 03/06~~ from 7:00 to 14:00 UTC on 03/06, and from ~~the~~
453 ~~04/06 at~~ 16:00 UTC on 04/06 to ~~05/06 at~~ 06:00 UTC on 05/06. For this latter case, a rain front (100
454 000 km²), moving eastward from Spain and North Africa regions, reached the FAST station the
455 night between the 4 and 5 June (Fig. 34). Wet deposition between the 4 and early 5 June in the
456 FAST station area were confirmed by radar imagery, showing several other instances of rain ~~spots~~
457 around the R/V position before and after the rain sampling (Fig. 34). Continuous on-board lidar
458 measurements confirmed the below-cloud deposition during the rain event of early 5 June (Fig.
459 2b3b). Rain FAST was a wet deposition event occurring at the end of an episode of transport of
460 Saharan dust, whereas precipitation ~~of~~on the 3 June occurred during the maximum of the dust
461 plume (Fig. 2b-3b and S2). The surface concentrations of gas and particles, measured on-board,
462 suggest no clear dust or anthropogenic influence in the atmospheric boundary layer during ~~the~~this
463 period of wet deposition, in agreement with back trajectories of low altitude air masses (Fig S2.),
464 presuming no local mixing between dust and anthropogenic particles into rain samples. The total
465 precipitation estimated from radar rainfall ~~estimates~~ yield an accumulated precipitation of 6.0 ± 1.5
466 mm (± 25 km around the R/V position), in agreement with ECMWF reanalysis ERA5 (Fig. S22) for
467 the wet deposition on the night of 4-5 June (5.7 ± 1.4 mm in the grid-point spanning the R/V position,
468 i.e. $\pm 0.25^\circ$ ~~around~~).

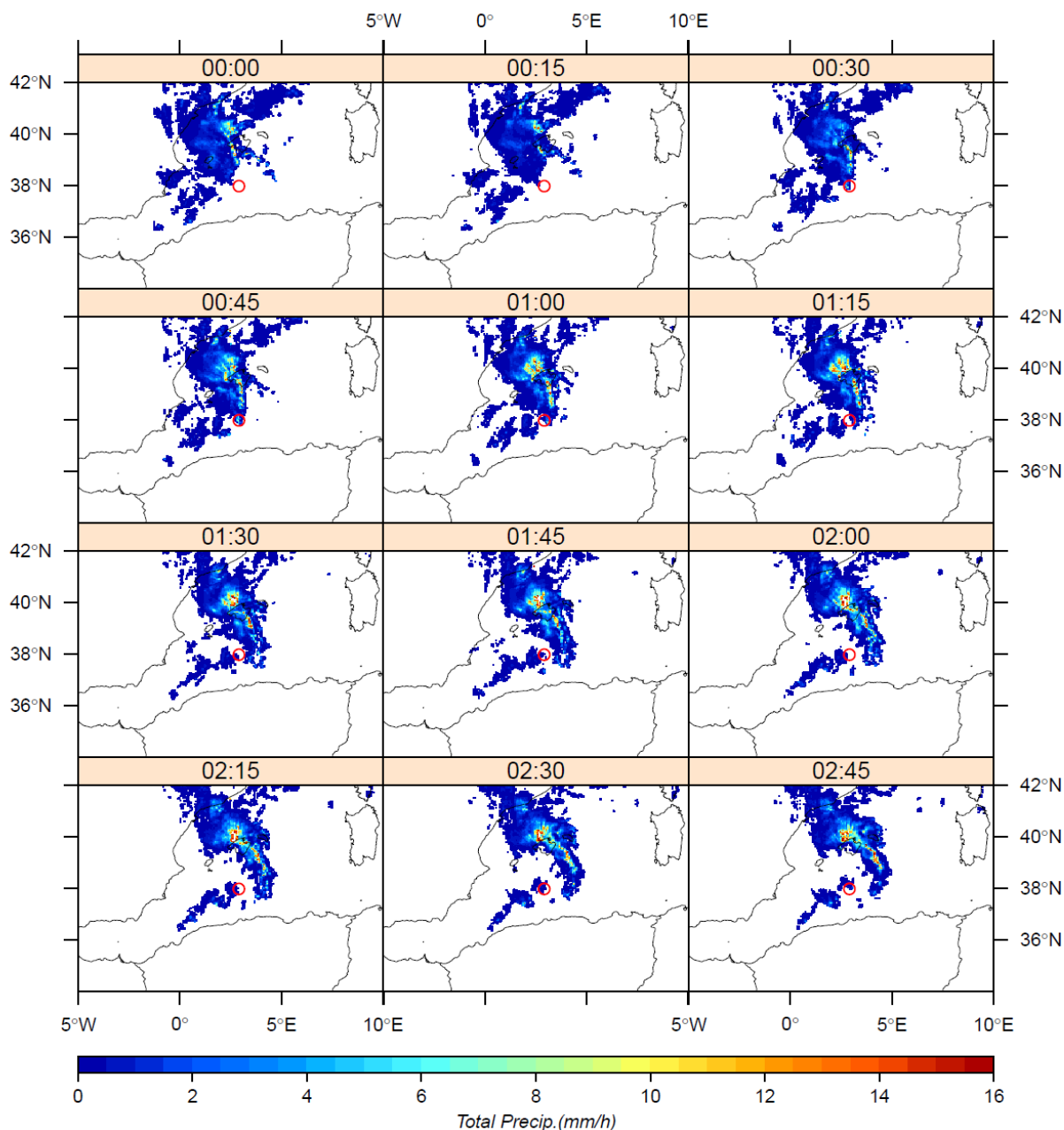


Figure 34: Rain rates (mm/h) during the night between the 4 and 5 June, when Rain ~~Fast-FAST~~ **has** ~~was been~~ collected on-board, issued from European rain radar composites (OPERA programme) of ~~5 June~~ **5** between 00:00 and 02:45 UTC.

3.2. Chemical composition of rains

Dissolved and total concentrations of nutrients and TMs in the rain samples are presented in Table 2. Among all measured dissolved concentrations, ~~NO₃~~ **nitrate** was the most abundant nutrient, followed by ammonium (Table 2). The nitrite concentration was ~~under~~ **below** the limit of detection for the two rain samples. Regarding TMs in rain, Fe and Zn presented the highest concentrations ~~in~~ **rain samples** with the same order of magnitude (10 to 25 $\mu\text{g L}^{-1}$). Co, Cd and Mo had the lowest

concentrations ($<0.1 \mu\text{g L}^{-1}$ in both events, associated to the greatest uncertainties due to LoD), whereas the other TMs concentrations ranged between 0.1 and $10 \mu\text{g L}^{-1}$ ~~in both rains~~ (Table 2). Concentrations of nutrients and the majority of TMs were higher in the dust-rich rain, except dissolved Pb (similar concentrations in both rain samples) and Cr (3 times higher concentration in Rain ION relative to Rain FAST).

Table 2: Dissolved and total concentrations of nutrients and TMs in the two rain samples collected during the PEACETIME cruise in $\mu\text{g.L}^{-1}$ or ng.L^{-1} and $\mu\text{mol.L}^{-1}$ or nmol.L^{-1} in the parentheses (sd = standard deviation from three replicates).

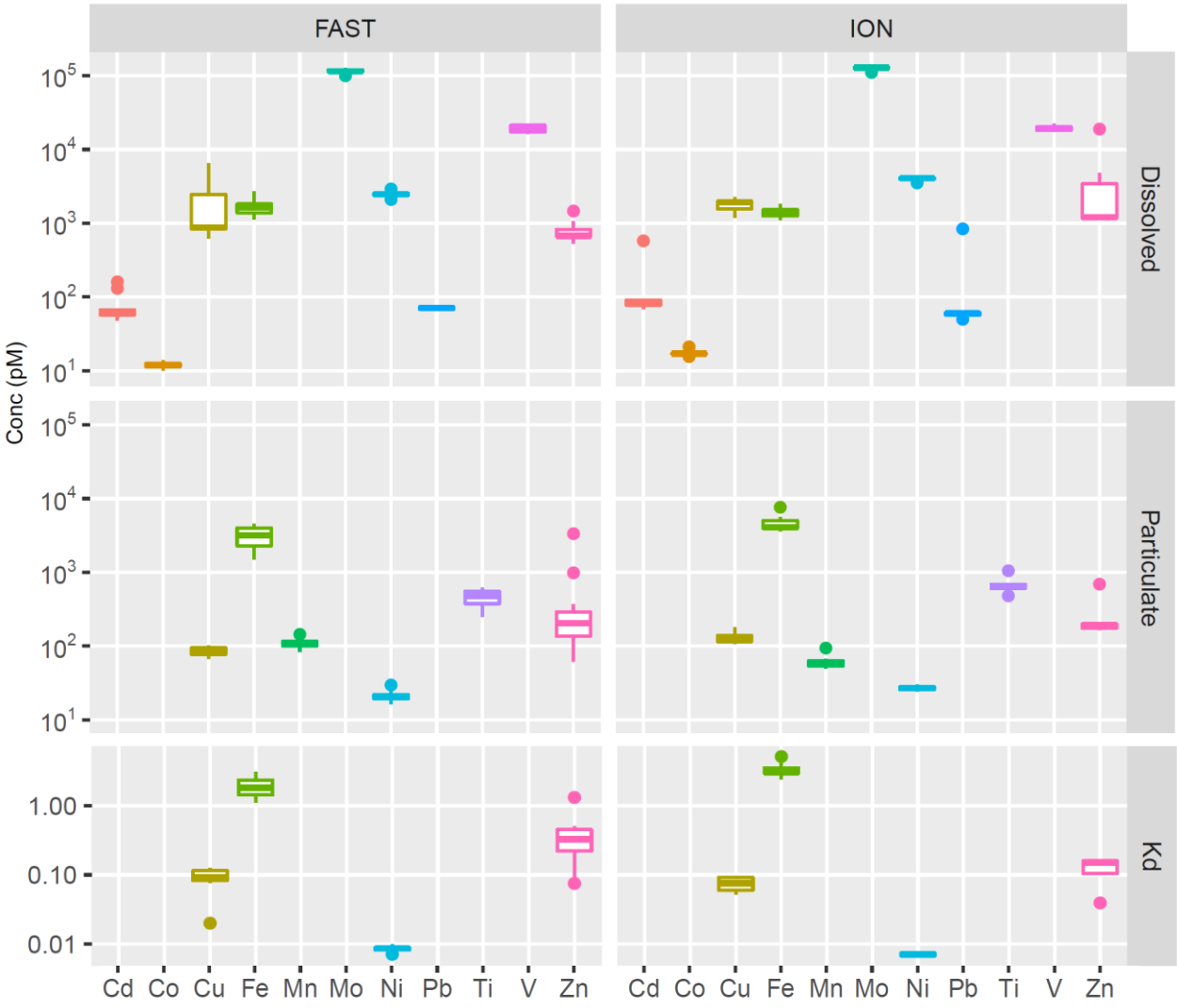
			Rain ION				Rain FAST			
			Dissolved		Total		Dissolved		Total	
			concentrations	$\pm sd$	concentrations	$\pm sd$	concentrations	$\pm sd$	concentrations	$\pm sd$
Nutrients	NO ₃ ⁻	μg L ⁻¹ (μmol L ⁻¹)	1185 (19.1)	71 (1.1)			3694 (59.6)	222 (3.6)		
	NH ₄ ⁺	μg L ⁻¹ (μmol L ⁻¹)	366 (20.3)	11 (0.6)			654 (36.3)	19 (1.1)		
	DIN	μg L ⁻¹ (μmol L ⁻¹)	552 (39.4)	82 (1.7)			1343 (96)	241 (17)		
	PO ₄ ³⁻	μg L ⁻¹ (nmol L ⁻¹)	18.1 (189)	0.5 (6)			19.0 (200)	0.6 (6)		
	DIP	μg L ⁻¹ (nmol L ⁻¹)	5.87 (189)	0.18 (6)			6.20 (200)	0.19 (6)		
	DOP	μg L ⁻¹ (nmol L ⁻¹)	8.63 (278)	1.94 (75)			4.91 (158)	1.56 (57)		
	TP	μg L ⁻¹ (nmol L ⁻¹)	14.51 (468)	2.52 (81)	16.6 (536)	1.0 (33)	11.11 (358)	1.95 (63)	58.7 (1894)	3.5
	DIN/DIP		(208)				(480)			
	DOC	(μmol L ⁻¹)	(105.7)	(2.2)			(95.5)	(1.2)		
Metals	Al	μg L ⁻¹ (nmol L ⁻¹)	13.0 (480)	0.8 (30)	14.6 (540)	0.9 (32)	23.4 (867)	0.7 (24)	440 (16308)	7
	Cu	μg L ⁻¹ (nmol L ⁻¹)	0.71 (11.1)	0.02 (0.3)	0.73 (11.5)	0.02 (0.3)	1.15 (18.0)	0.04 (0.6)	1.63 (25.7)	0.06
	Fe	μg L ⁻¹ (nmol L ⁻¹)	15.1 (270)	0.4 (6)	17.9 (321)	0.6 (11)	19.2 (344)	0.1 (2)	231 (4140)	7
	Mn	μg L ⁻¹ (nmol L ⁻¹)	0.55 (10.0)	0.02 (0.3)	0.60 (10.9)	0.02 (0.4)	3.17 (57.8)	0.07 (1.2)	5.26 (95.7)	0.12
	Ni	μg L ⁻¹ (nmol L ⁻¹)	0.52 (8.8)	0.02 (0.3)	0.67 (11.4)	0.02 (0.4)	0.59 (10.1)	0.02 (0.4)	0.84 (14.3)	0.03
	Ti	μg L ⁻¹ (nmol L ⁻¹)	0.48 (10.0)	0.04 (0.8)	0.65 (13.6)	0.48 (3.2)	0.22 (4.7)	0.01 (0.1)	33.36 (697)	0.51
	V	μg L ⁻¹ (nmol L ⁻¹)	0.37 (7.4)	0.01 (0.2)	0.38 (7.42)	0.01 (0.25)	1.37 (26.9)	0.03 (0.5)	2.02 (39.7)	0.04
	Zn	μg L ⁻¹ (nmol L ⁻¹)	24.8 (379)	0.8 (12)	25.3 (387)	0.8 (12)	22.7 (347)	0.6 (8)	26.3 (402)	0.7
	Cd	ng L ⁻¹ (pmol L ⁻¹)	12.9 (115)	6.4 (57)	13.1 (117)	6.3 (56)	20.2 (180)	10.3 (92)	23.7 (210)	6.8
	Co	ng L ⁻¹ (pmol L ⁻¹)	44 (749)	13 (229)	47.4 (804)	14.5 (246)	82 (1386)	20 (347)	157 (2661)	28
	Cr	ng L ⁻¹ (pmol L ⁻¹)	241 (4636)	16 (300)	628 (12079)	5 (95)	79 (1522)	14 (260)	443 (8514)	43
	Mo	ng L ⁻¹ (pmol L ⁻¹)	28 (288)	10 (106)	4.1 (43)	1.4 (14)	82 (855)	11 (113)	92.1 (960)	16.2
	Pb	ng L ⁻¹ (pmol L ⁻¹)	170 (822)	11 (54)	175.1 (845)	1.4 (7)	166 (801)	9 (41)	604 (2917)	19

3.3. Marine concentrations ~~and stocks~~

All the TMs had significantly higher concentrations in the ML compared to water below the ML and deeper (e.g. for Fe: Bressac et al., 2021 deep water masses), in agreement with a stratified profile associated with atmospheric inputs. The ~~particulate-pTM~~ and ~~dissolved-trace-metal~~TM concentrations within the ML (0-20 m) ~~and the SML~~ are displayed in Fig. 45. Concentrations were of the same order of magnitude ~~in the two studied at ION and FAST stations, except for the particulate phase in the SML where the concentrations of Cu and Co were significantly lower at ION station.~~ The TMs were mainly in dissolved forms in the ML (K_d from 0.006 to 0.5), except for Fe, ~~whose dissolved and particulate concentrations were in the same order of magnitude~~ (K_d around

2) and one outlier value for Zn (1.3) (Fig. 5). ~~On the contrary, the particulate phase contribution dominated for TMs in the SML, in particular at the ION station.~~

At both stations, the highest TMs concentrations in the surface seawater were found for dMo ~~in the dissolved fraction~~ (~120 nM), these values are the first measurements published in Med Sea and are in agreement with the high abundance of ~~dissolved~~-Mo in open seawater in other oceanic regions (~107 nM, Smedley and Kinniburgh, 2017). ~~and Fe is the most abundant~~ in the particulate fraction in the ML (~4 nM). All the ~~particulate-pTM and dissolved~~-TMs concentrations measured during the cruise were representative within the range previously published for the ~~Mediterranean~~ Sea (Sherrell and Boyle, 1988; Saager et al., 1993; Morley et al., 1997; Yoon et al., 1999; Wuttig et al., 2013; Baconnais et al., 2019; Migon et al., 2020, GEOTRACES-IDP2021). However, dCo concentrations (from 10 to 20 pM) were among the lowest ones measured during stratification period in Western Med Sea (~120 pM, Dulaquais et al., 2017). Zn presented the largest range of concentrations within the ML both in the ~~dissolved particulate and dissolved-particulate fractions~~ phases (0.6 to 19 nM and 61 to 3300 pM respectively), due to some high concentrations. However, the concentrations stayed in the typical range of values ~~found reported in the for the~~ Mediterranean Sea (Bethoux et al., 1990, Yoon et al., 1999), even if ,we cannot exclude a possible contamination for these outlier concentrations. ~~In the SML, the concentrations were lower than in the ML and Pb dominated both in dissolved and particulate phases. Tovar-Sanchez et al. (2020) showed that the TMs concentrations in the SML during the PEACETIME campaign were generally lower than those previously measured in the Mediterranean Sea, except in the particulate phase during the FAST station after dust deposition.~~



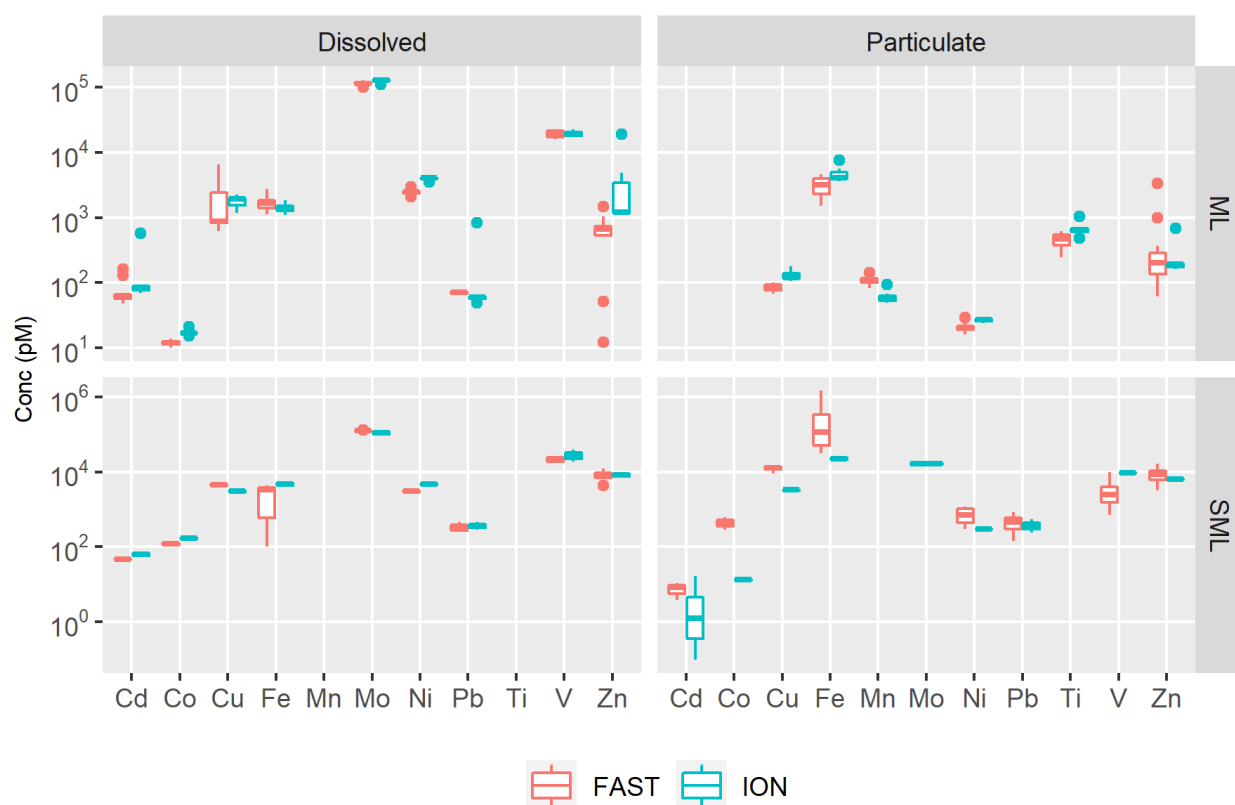


Figure 45: Box plots of dissolved (left upper panels) and particulate (right middle panels) marine concentrations (pM) and Kd values (lower panels) for the different TMs within the ML (upper panels) and the SML (lower panels) at ION (right panels) and FAST (left panels) stations. In the box plots, the box indicates the interquartile range, i.e. the 25th and the 75 th percentile, and the line within the box marks the median. The whiskers indicate the quartiles ± 1.5 times the interquartile range. Points above and below the whiskers indicate outliers outside the 10-th and 90th percentile.

4. Discussion

4.1. Composition of rain collected over the remote Mediterranean Sea

4.1.1. Concentrations

Regarding nutrients, nitrogen species concentrations in rain samples were in good agreement with those reported in Mediterranean rain samples, ranging from 1130 to 5100 $\mu\text{g L}^{-1}$ for NO_3^- and between 207 and 1200 $\mu\text{g L}^{-1}$ for NH_4^+ (Loye-Pilot et al., 1990; Avila et al., 1997; Al Momani et al., 1998; Herut et al., 1999; Violaki et al., 2010; Izquieta-Rojano et al., 2016; Nehir and Koçak, 2018). The FAST rain concentrations were within the average values published range, whereas the ION rain was in the low range, confirming a background signature at this station. The rainwater

536 samples presented a large dominance of N in comparison to P, as observed from the N/P ratio
537 derived from DIN/DIP (Table 2) ranging from 208 at ION to 480 at FAST. Previous observations
538 showed a predominance of N relative to P—in the atmospheric bulk deposition over the
539 Mediterranean coast, with average ratio higher than Redfield ratio (Markaki et al., 2010, Desboeufs
540 ~~et al., 2018~~). ~~The highest ratio about 100, the highest observed~~ reaching 170 for DIN/DIP and
541 1200 (in case of for DIN/TDP (Markaki et al., 2010, Desboeufs et al., 2018)), ~~but were on average~~
542 ~~around 100 in bulk deposition~~. The highest ratio could be linked to a washout effect of ~~the~~ gaseous
543 N species (~~as~~ NO_x and NH₃) by rain (Ochoa-Hueso et al., 2011). At the two stations, ~~no high~~
544 observed NO_x concentrations were under limit of detection ~~observed~~ in the boundary layer before
545 wet deposition. The presence of nitrate and ammonium in the background aerosols has been
546 ~~emphasized~~ observed during recent campaigns in the remote Mediterranean atmosphere (e.g. Mallet
547 et al., 2019). To our knowledge, no data are available on both P and N concentrations in
548 Mediterranean aerosols. The lowest concentrations of P relative to N in aerosol particles in the
549 Mediterranean ~~have been were~~ observed during the cruise (DIN/TDP ranged from 13 to 790, Fu et
550 al., in prep.). The TDP concentrations were consistent with the average value of 8.4 µg L⁻¹ measured
551 in African dust rain samples collected in Spain over the 1996-2008 period (Izquierdo et al., 2012).
552 Inorganic phosphorus predominated in the dust-rich rain, whereas organic P was dominant in the
553 background rain as the contribution of DOP to the TDP was 60% and 44% in Rain ION and Rain
554 FAST, respectively. The DOP/TDP ratio presents a very large range in Mediterranean rains,
555 spanning from 6% in Spanish dusty rain samples (Izquierdo et al., 2012) to 75-92% in rains from
556 Crete ~~Islands~~ (Violaki et al., 2018). A reason for this wide range could be that Mediterranean
557 European aerosols, as opposed to Saharan dust particles, are dominated by organic phosphorus
558 compounds associated with bacteria (Longo et al., 2014).

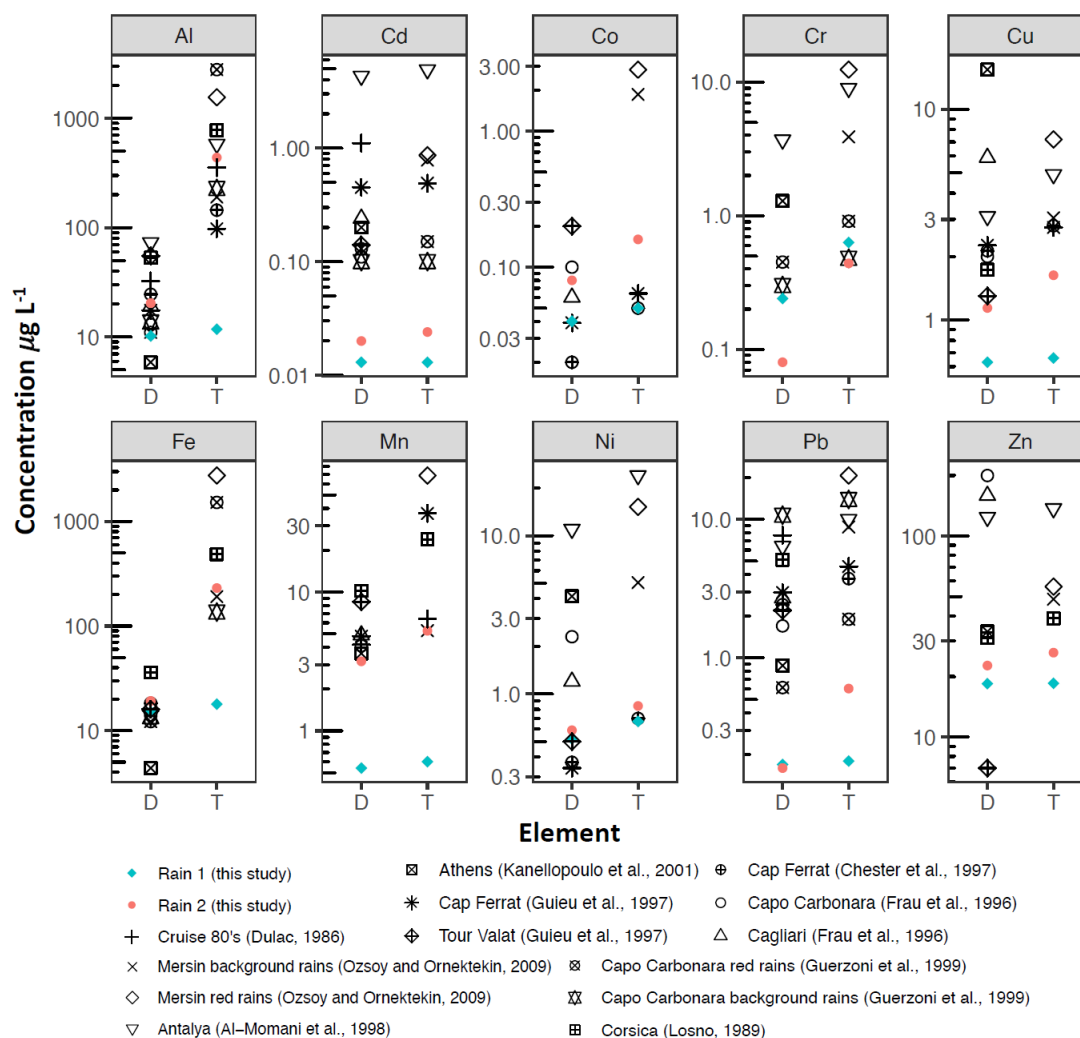


Figure 56: Comparison of dissolved (D) and total (T) TMs concentrations along with data from 14 former to previous studies carried out in the eastern and western Mediterranean Sea.

The dissolved and total TMs concentrations in the PEACETIME rains were lower than those reported in coastal areas (eastern Basin: Özsoy and Örnektekin, 2009; Al-Momani et al., 1998; Kanellopoulou et al, 2001 and western Basin: Guieu et al., 1997; Guerzoni et al., 1999b; Chester et al., 1997; Losno, 1989; Frau et al., 1996) (Fig. 5), notably especially for the background Rain ION (Fig. 6). Most of the referenced works on coastal rainwaters date from the late 1990s. There is a continuous decline of TM emissions since 90's due to regulatory efforts (Pacyna et al., 2007). The subsequent decrease of the anthropogenic Cd and Pb imprint on atmospheric inputs from European coasts to open sea is well documented (OSPAR, 2008; Travníkov et al., 2012; Geotraces IDP21). Since the phasing-out of leaded automobile gasoline, the decrease of atmospheric Pb concentrations is also observed in Mediterranean atmosphere (Migon et al., 2008). The low TM concentrations of ION and FAST rain samples, in particular Cd and Pb, suggest a pronounced decrease of TM inputs

in open Mediterranean due to environmental mitigation on TM emissions. Moreover, the coastal deposition is generally not representative of open sea inputs, e.g. due to proximity of anthropogenic sources in coastal areas. Thus, the 90's data should not be used as a current reference for open Mediterranean rain composition. This suggests the probable effect of both local anthropogenic influence at coastal sites due to higher aerosol concentrations in comparison to remote Mediterranean (Fu et al., in prep.) and due to the reduction of anthropogenic emission for some elements since most of the referenced works on coastal rainwaters date from the late 1990s. This is particularly true for Cd and Pb whose emissions have strongly decreased over the last decades, notably due to removal of lead in gasoline and reduction of coal combustion (Pacyna et al., 2007). This has resulted in a clear decrease in the particulate concentrations of these metals in the Mediterranean atmosphere (Migon et al., 2008), consistent with the fact that concentrations in the PEACETIME rains are one to two orders of magnitude lower than reported in the literature. For these metals, the discrepancy is also observed between the concentrations in our open-sea rain samples and the concentrations measured in three rains collected at sea in April 1981 (Dulac, 1986), confirming the large decrease of concentrations could be related with the decrease of emission. Thus, our results show the former literature cannot be used as current reference about coastal rain composition due to recent environmental mitigation on metals emissions.

4.1.2. Enrichment factor

EF and solubility values of TMs and P observed during the two rain events were very contrasted (Fig. 67). In Rain ION, almost all elements were significantly enriched relative to ~~earth~~ the upper continental crust ($EF > 10$, and up to $\sim 10^3$ for Cd and Zn), whereas in Rain FAST, only Zn (73), Cd (48) and Mo (15) were ~~slightly~~ enriched. Only Ti, Fe, and Mn did not present a significant enrichment ($EF < 10$) in Rain ION, in agreement with previous studies in the Mediterranean environment showing that these metals are mainly associated with mineral dust in ~~atmospheric~~ deposition (e.g., Guieu et al., 2010; Desboeufs et al., 2018). Yet, for Fe and Mn, an influence of non-crustal sources in Rain ION could be suspected through a clear increase in the EF values compared to FAST. Mo is the most abundant TM in seawater (Smedley and Kinniburgh, 2017) and in particular in Med Sea (see section 3.3). Thus, at the difference of other TMs, the non-crustal part of Mo could be associated to seasalt aerosols rather than anthropogenic signal. The EF ratio relative to seawater ($(Mo/Na)_{seawater} = 8.9 \cdot 10^{-7}$ in mass ratio, Millero, 2013) were 7.4 for Rain ION and 4.6 for Rain FAST confirming the marine origin of this element in both rain samples. ~~Both rains, EF of Zn was in average five times higher than EF found in the rains previously studied in the Mediterranean region (Özsoy and Örnektekin, 2009; Al Momani et al., 1998; Losno, 1989).~~

~~However, extremely high enrichments of Zn in rainwater have also been reported by Frau et al. (1996) with a geometric mean EF of about 6500 in both crust rich and crust poor rains from two sites in southern Sardinia. Fu et al. (2017) also reported EF higher than 1000 for Zn in atmospheric bulk deposition in Lampedusa Island.~~ The anthropogenic origin of ~~particulate~~ TMs and P have been reported by several studies on atmospheric deposition monitoring in the western Mediterranean (e.g., Guieu et al., 2010; Sandroni and Migon, 2002; Desboeufs et al., 2018). For example, Desboeufs et al. (2018) showed that there is a large contribution of anthropogenic combustion sources ~~in to the~~ P, Cr, V and Zn background deposition fluxes. Aerosol composition monitoring over the Mediterranean coastal area showed the role of land-based sources and ship traffic sources on TMs contents (Bove et al., 2016; Becagli et al., 2017). ~~However, As~~ all these ~~sampling deposition measurements~~ sites were located in coastal areas, ~~where~~ it was difficult to ~~discriminate the potential local influences~~ exclude the influence of these local sources for explaining the observed anthropogenic contribution. Here, EF values showed a clear anthropogenic signature for P and all TMs except Ti, Fe, Mn and Mo in the offshore Rain ION sample. In particular, the EF of Zn in Rain ION was on average five times higher than the EF found in the rain samples previously studied from coastal sites in the Mediterranean region (Özsoy and Örnektekin, 2009; Al-Momani et al., 1998; Losno, 1989). Nevertheless, extremely high enrichments of Zn in rainwater have been reported from island sites in the Med Sea, for example Frau et al. (1996) reported geometric mean EF of ~6500 in both dust-rich and dust-poor rains from two sites in southern Sardinia, and Fu et al. (2017) reported EF >1000 for Zn in atmospheric insoluble bulk (wet+dry) deposition on Lampedusa Island. As previously discussed (section 3.1.1.), Rain ION was representative of a Mediterranean background marine rain event. The Zn EF at station ION was the same order of magnitude as at these island sites which suggests a high anthropogenic background signal of Zn even in open Med. More generally, even if the on-board atmospheric gas and particle measurements did not show a specific anthropogenic influence during the period of Rain ION, the particles scavenged by this rain presented a clear anthropogenic signature for all TMs except Ti, Fe and Mn; however for Fe and Mn, an influence of non-crustal sources in Rain ION is visible through a clear increase in the EF values compared to FAST (Fig. 6). This high EFs in Rain ION means that even over the remote Med Sea, the chemical composition of background aerosol particles is likely continuously impacted by anthropogenic sources.

~~Moreover, t~~ The EF values of TMs for Rain FAST were significantly lower than for Rain ION (Fig. 67) but similar to Saharan rains (Guerzoni et al., 1999b; Özsoy and Örnektekin, 2009), confirming

the dust signature for this rain. The comparison between dust-rich and background rains generally reveals a net difference of concentrations (at least higher by a factor 3 in dust-rich), notably for Al, Fe, Mn and Cr (Guerzoni et al., 1999b; Özsoy and Örnektekin, 2009). Here, an increase in concentrations between rains ION and FAST was observed. Such contrast was indeed observed for the majority of TMs: Al (x28), Ti (x50), Mo (x23), Fe (x13), and Mn (x9) in the PEACETIME rains (Fig. 5), but also for Cu and V (x5), Pb (x3.5), Co(x3) and Cu (x2) but also for P(x4) (Table 2). The combination of higher concentrations and EF values <10 found in Rain FAST ~~confirm~~ show that the dust contribution was important on deposition fluxes of many TMs and P during this event. However, the high Al concentrations in rain FAST drives mathematically down EF values, masking potentially other source signature.

4.1.3. Solubility

The solubility values were also ~~larger~~ higher in Rain ION than in the dusty Rain FAST, except for Mo for which the difference between both rain samples ~~wais~~ not significant (Fig. ~~67~~). For Rain ION, TMs and P presented solubility higher than 78%, except for Cr (38%). In Rain FAST, solubility values <10% were observed for Al and Fe, more than 10 times lower than in Rain ION. For the other TMs, the highest difference in solubility was observed for Pb whose solubility decreased from 97% in Rain ION to 27% in Rain FAST. In a review on TMs solubility in Mediterranean rainwaters collected in coastal areas, Desboeufs (2021) emphasize the large range of solubility for all the TMs: Fe (0.8-41%), Cr (6-80%), Pb (5-90%), Ni (22-93%), Mn (16-95%), Cu (22-96%), Zn (14-99%), V (35-99%) and Cd (72-99%). The solubility ranges found in this study were generally consistent with those reviewed by Desboeufs (2021). ~~In particular~~ Moreover, the Mn solubility values in FAST (60%) and ION (92%) rains are close to those reported by Dulac (1986) from a dust-rich (57%) and an anthropogenic (83%) rain collected at sea in the Ligurian Sea and west of Sardinia in April 1981, ~~respectively~~. Only Fe solubility (84%) found in Rain ION was higher than the average values previously reported. In the Rain FAST, Fe solubility was 8%, this is 10 times lower than the average Fe solubility in 10 dust-rich rains collected on the southeastern coast of Sardinia by Guerzoni et al. (1999b), but consistent with Saharan dust ~~wet~~ deposition collected in the Atlantic Ocean (~~Chance et al., 2015; Powell et al., 2015~~ Sedwick et al., 2007; Baker et al., 2017-2013). It is known that anthropogenic Fe is more soluble than Fe-bearing dust (Desboeufs et al., 2005, Jickells et al., 2016). Regarding the evolution of TM emissions (see section 4.1.1), we suspect that this difference could be due to a higher contribution of anthropogenic signal for Fe in dust-rich rains in 90's in Sardinia that in the recent rain samples.

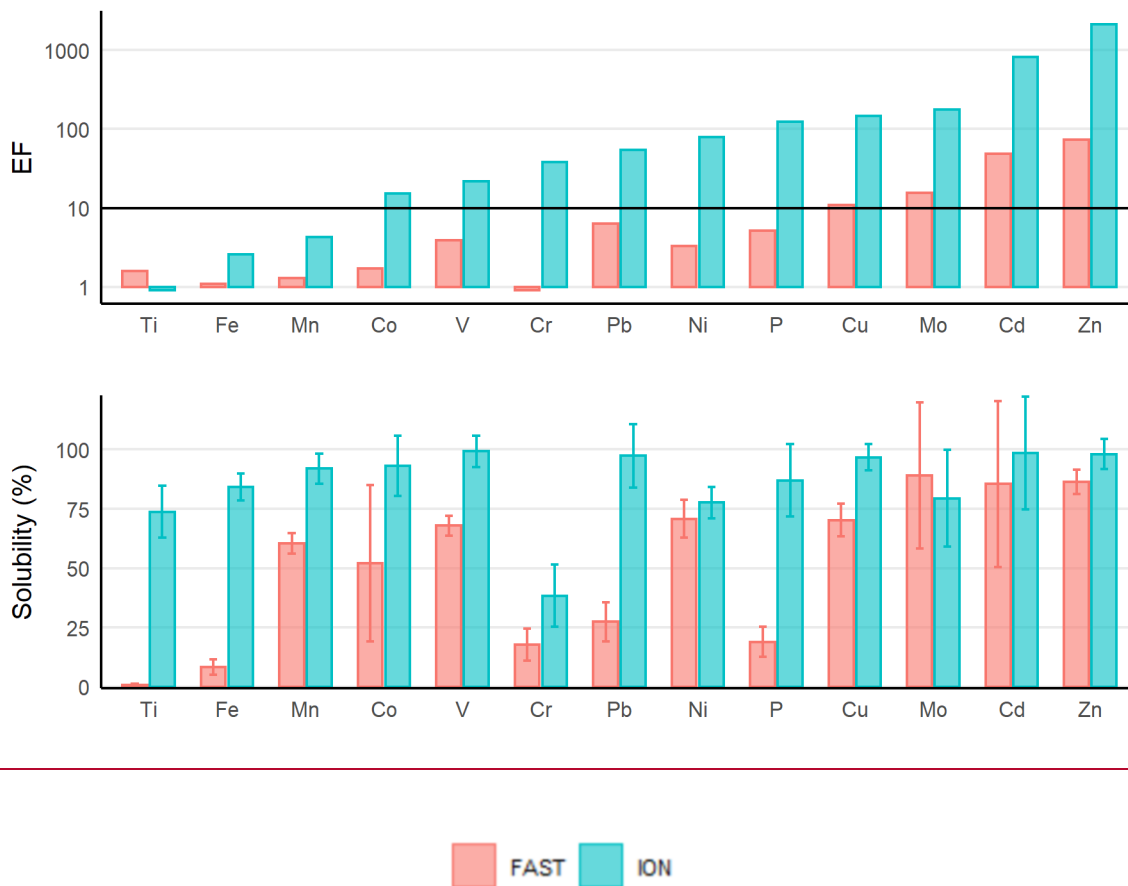


Figure 67: Enrichment Factors (EF, upper panel) and solubility (% , bottom panel) of phosphorus (P) and TMs ordered by increasing EF in the two rainwater samples.

Few studies have compared TMs solubility between dust-rich and background-anthropogenic rains in Mediterranean-in-the-Mediterranean. In Sardinia, Guerzoni et al. (1999b) observed an increase in solubility values from dust-rich to background rains was observed for Mn in offshore rains as mentioned above (Dulac, 1986) and for Al, Cr, Fe and Pb (and hardly but only a slight increase for Cd) in Sardinia (-Guerzoni et al., (1999b)-observed). The decrease in solubility from background to dust-rich rains was observed for P in Spain by Izquierdo et al. (2012), with values of solubility decreasing from 25% to 7%. Here, our results on the two rain samples confirm the lowest solubility of TMs in dust-rich rains (except for Mo). Aerosol leaching experiments showed that, and reported an inverse relationship between the particle concentration and solubility of Al, Fe, Pb and Cd. Similarly, Theodosi et al. (2010) showed a decrease in TMs solubility with the increase in dust load in rains collected on Crete Island. In those two studies, this decrease was dependent on the considered metal, with Pb presenting the highest decrease in solubility. The decrease in solubility from background to dust-rich rains was also observed for P in Spain by Izquierdo et al. (2012), with values of solubility decreasing from 25% to 7%, and for Mn in offshore rains as mentioned above (Dulac, 1986). Metal partitioning in rainwater dissolution from aerosol particles

can be also influenced by a number of parameters, such as pH, presence of dissolved organic complexing ligands, in-cloud ~~processes~~processing, particle origin and ~~origin and~~-load (Desboeufs et al., 1999; Bonnet and Guieu, 2004; Desboeufs et al., 2005; Paris and Desboeufs, 2013; Heimbürger et al., 2013, Jickells et al., 2016). Regarding metal partitioning in rainwater, the role of pH and of ~~However, the~~ particulate ~~desert-mineral~~ dust loading, reflecting the dust versus anthropogenic signature, ~~is-were identified as the main the main controls~~ of TMs solubility in the Mediterranean rainwater (Özsoy and Örnektekin, 2009; Theodosi et al., 2010). From our two rain samples, it is difficult to propose a control explaining the difference in solubility values. However, the pH values were very close in the two samples (Table 2), excluding a pH effect on solubility values. A much lower solubility of TMs in Rain FAST is consistent with the EFs indicating a crustal origin of TMs in Rain FAST (Fig. 6). As discussed before, background atmosphere in Med Sea seems to be continuously influenced by anthropogenic particles. Even in dusty-rain FAST, it is highly probable that a part of metals presented an anthropogenic imprint, not visible on EF values but with solubility similar than in Rain ION. Thus, the decrease of solubility between the two rain samples could be either due to the lowest solubility of TMs in mineral dust (as suggested by aerosol leaching experiments), either results from the presence of mineral dust which by increasing the TM total concentrations overwhelms the anthropogenic background signal, or both. A much lower solubility of TMs in Rain FAST than in Rain ION (except for Mo) is consistent with the EFs in Rain FAST (Fig. 6), although no correlation between solubility and EF values could be observed. The case of Mo is unique, since its solubility was comparable in Rains ION and FAST ~~despite a >20 times higher EF in Rain ION.~~ As discussed from EF values Mo was associated to seasalt aerosols in both rain samples, explaining the similarity of solubility. As Mo solubility is seldom studied in the literature, we could not conclude on the reason for this particular outcome. It is interesting to note that despite the desert signature, the majority of metals have solubility greater than 50% in rain FAST.

4.2. Atmospheric wet deposition as a source of TMs to the surface seawater

4.2.1. Atmospheric fluxes

As mentioned before, the two collected rains were part of large rain systems, associated with patchy rainfalls that lasted several hours or days (see section 3.1). This spatio-temporal variability led to heterogeneity in both rainwater concentrations and accumulated precipitation across the studied region. Such spatial variability has been observed by Chance et al. (2015) in the Atlantic Ocean. Moreover, even weak lateral advection can transfer surface water impacted by intense precipitation

721 in the vicinity of the vessel. On this basis, the spatial extrapolation of wet deposition fluxes seems
722 subject to ~~a~~ large uncertainty ies (almost 100% RSD) when the rain samples are not collected across
723 the rain area (Chance et al., 2015). To best counteract this effect, spatial variability was taken into
724 account to quantify ~~the~~ total precipitation i.e. 3.5 ± 1.2 mm for rain ION and 6.0 ± 1.5 mm for rain
725 FAST (see section 3.1) in order to quantify the wet deposition fluxes (here ~25% RSD for total
726 precipitation and 1 to 74% RSD for concentrations).

727 From the total (dissolved + particulate) Al concentration measured in the Rrain FAST sample, we
728 estimated the wet mineral dust deposition flux at 65 ± 18 mg m⁻², assuming 7.1% Al in dust (Guieu
729 et al., 2002). The vertical distribution of dust particles (Fig. 2b3b) and the absence of high Al
730 concentrations close to the sea surface (Fu ~~et al., in prep.~~ personal comm.) indicate that dust dry
731 deposition can be neglected. Based on the increase in total Al in the upper 20 m of the column water
732 following the deposition events and using 7.1% for Al in dust, Bressac et al. (2021) derived an
733 average dust deposition flux of ~ 55 mg m⁻² at FAST station, which is comparable to our estimate.
734 Although low compared to deposition fluxes reported in the western Mediterranean (Bergametti et
735 al., 1989; Lojze-Pilot and Martin, 1996; Ternon et al., 2010), ~~such our flux values estimates~~ are
736 among in the same order of magnitude of the most intense weekly dust deposition fluxes ~~recorded~~
737 calculated more recently in Corsica between 2011 and 2013 (14% of fluxes >50 mg m⁻²) and is
738 ~~equivalent comparable~~ to the mean weekly flux (93 mg m⁻²) ~~observed reported in for~~ Majorca
739 ~~Island~~ during the same period (Vincent et al., 2016). The ~~aerosol~~ columnar aerosol concentration
740 during the dust event at the FAST station being estimated to be between 0.18 and 0.24 g m⁻² (see
741 section 3.1.), the expected maximum values of atmospheric dust flux could be in this range. The
742 comparison with the estimated flux indicates that the atmospheric column was probably not totally
743 washed-out by the short rain event. Indeed, Fig. 2b-3b shows that a significant depolarization was
744 observed immediately after the rain ended on the ship R/V, before atmospheric advection could have
745 brought dusty air possibly not affected by rain. Satellite products (Fig. S2) confirm that on 5 June,
746 the dusty air mass was transported farther to the north-east from the station where it was replaced
747 by clear air.



Figure 78: Dissolved (upper panels) and particulate (lower-middle panels) wet deposition fluxes ($\mu\text{mol m}^{-2}$), and K_d (lower panels) for the different TMs estimated from the two rains sampled on-board, considering the standard deviation on the TMs concentrations and the spatial variability of total precipitation over the area of sampling (Rain ION in blue and Rain FAST in red). Note different scales on the y axes and that K_d value for Ti (115) in Rain FAST is out of scale.

The atmospheric dissolved and particulate wet deposition fluxes of TMs, derived from the chemical composition of rain samples and total precipitation of rain samples, are presented in Fig. 78. Co,

Mo and Cd presented the lowest fluxes in the two rainfalls. Zn and Fe fluxes were in the same order of magnitude and were the highest dissolved fluxes compared to the other TMs in the two rains. The comparison showed that almost all the dissolved TMs fluxes were higher in the dusty rain, except Cr and Ti. For the particulate phase, the fluxes were mainly increased by dust deposition for Co, Fe, Mn, Pb, Ti and V. The K_d values (0.1 < K_d < 1), in consistence with solubility values higher than 50% (Fig. 7), show that whatever the rain sample, the atmospheric TM inputs were, mainly dissolved, except Fe, Pb and Ti in Rain FAST and Cr in the two rains (Fig. 8). The comparison shows that almost all the dTM fluxes were higher in the dusty rain, except Cr and Ti due to their low solubility in Rain FAST. Our results emphasized suggest that dust deposition, even here in case of a moderate deposition flux, enabled resulted in higher atmospheric inputs of TMs than from a low perturbed-anthropogenic background rain, even here in the case of the moderate deposition input flux reported. With more than an order of magnitude difference in deposition fluxes in the two rain events, This this most is notably notably be the case for particulate Fe, Mn, Pb and Ti, typically poorly soluble from desert dust source. Dissolved Cd, Co, Cu, Mn and V fluxes present the highest increases between background Rain ION and dusty Rain FAST for dissolved Cd, Cu, Mn, V and Zn and for particulate Fe and Ti with more than one order of magnitude fluxes difference between the two rains. Yet, these former elements (except Mn) are usually considered issued from anthropogenic sources. The orders of magnitude found in this study could be used as a benchmark “typical atmospheric fluxes” to estimate atmospheric inputs of TMs by a rain event from wet deposition to the western Med Sea. However, We must keep in mind, however, that annual and long-term deposition fluxes of desert dust-related elements, as Fe, Mn and Ti (e.g. TERNON et al., 2010), but also nitrogen species (e.g., Richon et al., 2018b), in the Med Sea, are dominated by a few atypical intense deposition events in the Med Sea, when they occurred as is the case in many other oceanic regions (Duce et al., 1991).

4.2.2. Comparison between TMs wet deposition inputs and marine stocks at ION and FAST stations

As previously discussed, the atmospheric concentrations measured in this study were the most recent measurements in remote Med Sea, and were inferior to 90's measurements in coastal zone. As described in Guieu et al. (2020), marine dynamic conditions at FAST were favourable to observe any change in the water masses strictly attributed to external inputs coming from the atmosphere on a short time scale. Marine sampling sequences carried out before and after rains were, to our knowledge, the first direct observations to trace the fate of atmospheric metals and nutrients in the water column after wet deposition event. The time chart of the sampling of rain and column water (surface microlayer, subsurface seawater and mixed layer) is presented in Fig. 8. The impact of the

~~two-dust~~ wet depositions on nutrients stocks in the Mediterranean surface waters is discussed in details in van Wanbeke et al. (2020) and Pulido-Villena et al. (2021). To briefly summarise, ~~B~~ both nitrate and DIP increased in the ML following the rains. Although the closure of the N and P budgets had to necessarily take into account post-deposition processes such as new nutrient transfer through the microbial food web (uptake, remineralisation, and adsorption/desorption processes on sinking particles), it was shown that wet deposition was a significant source of nutrients for ML during the cruise. For example, atmospheric supply of phosphate could contribute to 90% of new production at FAST (Pulido-Villena et al., 2021). Bressac et al. (2021) studied the response to Al and Fe cycles to dust deposition during the cruise. They showed that total Fe and Al stocks were increased by dust wet deposition, and that the dissolved Fe atmospheric inputs were transient in the ML and were accumulated in the subsurface waters (100-1000m). The low depth-resolution of marine TM concentration samplings prevent the possibility to make TM inventories on the water column. We focus here on the role of dust TMs-wet deposition events as a source of ~~metals-TMs~~ to the ~~column surface water~~ mixed-layer, except Mo due its marine origin in the rain samples. The deltas of TM stocks before and after Rain FAST compared to the atmospheric fluxes are presented in Fig. 9. ~~To do so, we estimated the potential enrichment of SML and ML from the rain by calculating the difference (delta) in TMs stocks before and after rains.~~

~~At ION, no SML sampling was done after rain, preventing the study of the rain-effect. For ML, the large variability in total and dissolved stocks between the two casts ML25 and ML27 before the rain makes the establishment of a background concentration levels before rain difficult. ML27 was used as initial conditions since it is the closest sampling from post-rain measurements (ML29). As mentioned previously, dust rain deposition over the FAST station area started on 3 June. Bressac et al. (2021) showed that the dust signature, traced by changes in Al and Fe stocks in the ML, was already visible from the ML03 sampling. We defined the enrichment of seawater layers as the difference between the maximum stocks after rains (from SML 04 or 06 and ML05+4) and the initial seawater stocks (SML02 and ML02).~~

After Rain FAST, At ION, only particulate Cu (+27%) and Zn (+44%) stocks increased in the ML after the rain. Even if the dissolved forms of Cu and Zn predominated in the ML, this increase was accompanied by increasing K_d values, i.e. in the particulate/dissolved partitioning (0.07 vs 0.12 for Cu and 0.14 vs 0.2 for Zn). This was also the case for Fe (K_d increased from 2.6 to 4.3), although no significant difference (<5%) was observed on the particulate Fe stock. The K_d values in the ION rain sample being higher than in the marine stock before the rain, that suggests the wet deposition at ION is mainly an additional source of particulate TMs.

At FAST, In the SML, the dissolved and particulate stocks increased following rains for all TMs, from a factor 1.5 (Mo) to 10 (Fe) for the dissolved phase and from a factor 1.6 (Ni) to 67 (Fe) for the particulate phase (Fig. 9). the ML stocks increased in the particulate phase for pFe (+61%), pMn (+15%), pTi (+23%) and pZn (+9%) and in the dissolved phase for dCu-Co (+96%) and dFe (+46%), Pb (+8%) and Zn (+15%) (Fig. 9). The behaviour of pFe, pMn, pTi and pZn is consistent with observations on pAl stock which increased by 78% after rain (Bressac et al., 2021). In addition of marine inventories, The atmospheric particulate inputs were higher to the marine particulate deltas for all the TMs (Fig. 9), supporting that the marine stock increases resulted from atmospheric inputs. The particulate TMs inputs by rain in ML was also observed on from Kd increase in ML for Fe (values and total X/Al in the ML. For example, Kd(Fe) increased from 0.141.7 to 1.90.17 in ML and its Kd was 0.25 in the rain) and for Zn (0.33 to 0.57), in agreement with the highest Kd values in rain fluxes (Fig. 7) relative to marine ratio (Fig. 4). The increase Kd was even observed for Cu (0.044 to 0.091) and Ni (0.0081 to 0.0086). Even for Ni for which no change in stock could be evidenced, Kd(Ni) decreased from 0.1 to 0.07 and its Kd in the rain was 0.006. For Mn/Al It is probable that the rain inputs for these TMs be masked in the uncertainties of stock estimations. As dissolved concentrations of Mn and Ti were not measured in the ML, it is not possible to estimate the Kd values. However, the particulate Mn/Al which ratio fell from 0.27 before the rain to 0.008 after the rain (ML05+4), in accordance with the rain ratio (0.004002), confirming the impact of rain inputs on marine particulate stocks of Mn and Al. For Ti, the particulate Ti/Al ratios were very close in the ML (0.048) and in the rain (0.045), making it impossible to observe a rain effect. Here, the observed deltas were inferior to the rain inputs. However, the marine sampling were 4h after rain. Bressac et al. (2021) showed a decrease of 40% of pAl signal in 24h which could be explained either by a rapid settling of dust in the ML, or by lateral advection. The dynamic of pFe, pMn and pTi stocks, with a decrease with time after rain (not shown), is consistent with dust removal in the ML. The pCu and pNi inputs represented 4% and 10% of particulate marine stocks. The dust removal could overwhelm the signal of enrichment of these metals. However, we cannot exclude that the pCu and pNi inputs were masked by the uncertainties of stock calculations.

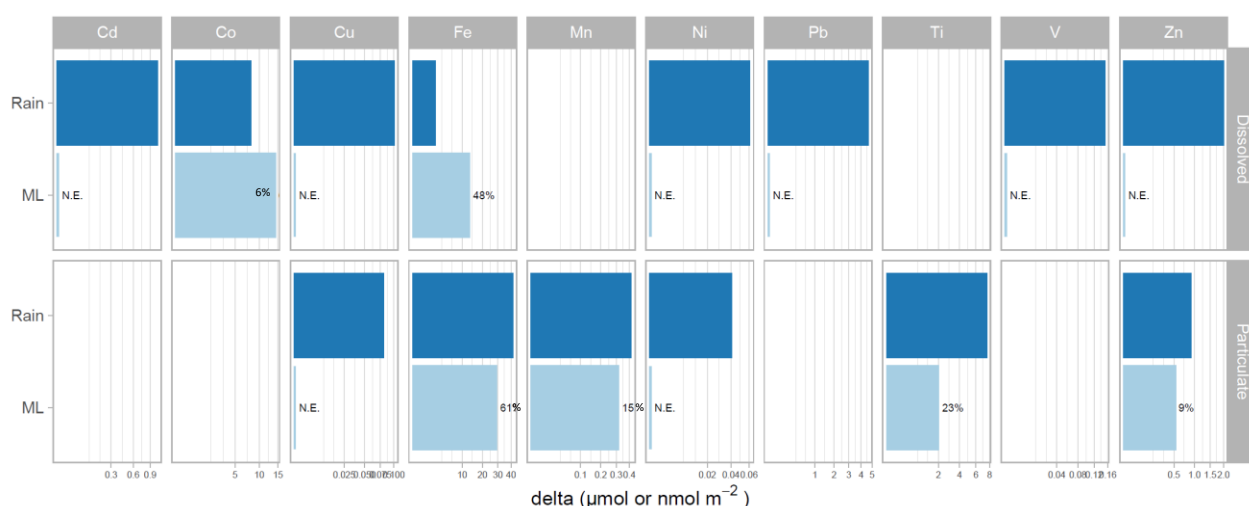
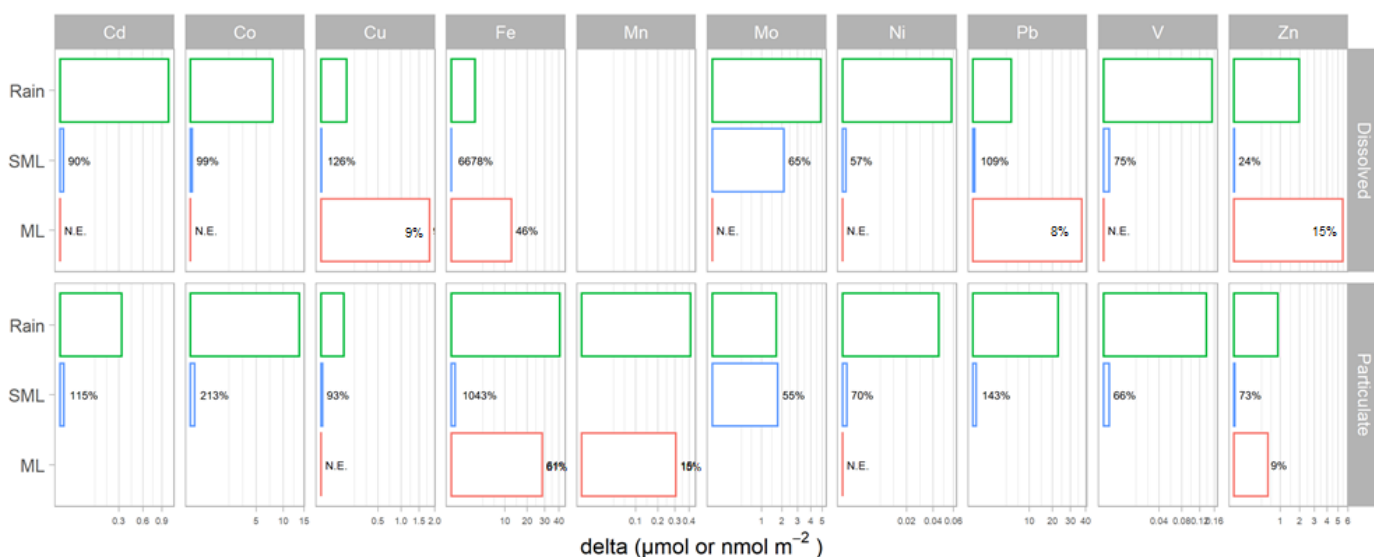


Figure 9: Comparison between TMs wet deposition fluxes (in green) and TMs marine stock deltas (before and after the rain) in the SML (in blue) and in the ML (in red) at FAST. Dissolved = upper panels and particulate = lower panels. Marine stocks increase are expressed in absolute values (Cd, Co and Pb stocks and fluxes in nmol m⁻², and the other TMs in μmol m⁻²) and in relative values (%). N.E.: not enhanced (increase <5%).

The comparison between the observed enhancements in the SML stocks and the rain inputs at FAST (Fig. 9) indicates that the atmospheric fluxes support all observed deltas. Indeed, the atmospheric particulate and dissolved fluxes of TMs were 2 to 4 orders of magnitude higher than the mean stocks present in the SML, except Mo which was in the same order of magnitude. In the ML, the magnitude of atmospheric particulate inputs was higher or similar to the particulate marine delta of Fe, Mn and Zn. For dissolved stocks, Cu, Fe, Pb and Zn, the increase in dissolved stocks within the ML was 2 to 10 times higher than what could provide the atmospheric inputs. no enrichment was observed for

Cd, Cu, Ni, Pb and Zn. This is not surprising for Cd, Cu, Ni, Pb and V since atmospheric dissolved inputs represent less than 1% of marine stocks. As expected from the comparison between inputs and stocks before rain, the marine dCo and dFe stocks were increased after dust deposition. However, the marine deltas within the ML for Co and Fe was 2 and 7 times higher than what could be provided from the atmospheric dissolved inputs. ~~As described in Guieu et al. (2020), marine dynamical conditions at FAST were favorable to observe any change in the water masses strictly attributed to external inputs coming from the atmosphere on a short time scale. However, A lateral transport and~~ a cumulative effect of previous and surrounding wet deposition events (from 3 June) could explain this ~~difference between atmospheric inputs from rain FAST and increase of marine dissolved stocks~~ positive mismatch. Several removal processes occurring in the ocean, such as biological uptake (Morel et al., 2003; Noble et al., 2008), passive scavenging by adsorption onto particles (Wuttig et al., 2013, Bressac and Guieu., 2013, Mackey et al., 2015; Migon et al., 2020) or chemical processes as precipitation (Wagener et al., 2010, Ye et al., 2011) are known to decrease dissolved TM concentrations in the first 24 or 48 hours after atmospheric deposition. During the cruise, Bressac et al. (2021) show that dust deposition represented a significant input of dissolved Fe in the ML only on a timescale of hours, due to scavenging or precipitation processes. It is highly probable that these removal processes limited the cumulative effect of dTM inputs. A post-deposition dissolution of Fe and Mn in seawater ~~could occur over several hours or days~~ was reported during dust seeding experiments simulating wet dust deposition in mesocosms over several hours or days (Wagener et al., 2008; Wuttig et al., 2013; Desboeufs et al., 2014). Mackey et al. (2015) show that in case of dry deposition, aerosol Co and Fe dissolution in seawater can be gradual and continue up to 7 days after contacting seawater. Considering the excess of TMs in marine stocks relative to rain inputs, our observations are consistent with the dissolution of Co and Fe in surface seawater following the first hours after wet dust deposition. Tovar-Sanchez et al., (2020) proposed that UV irradiation and the enrichment in organic matter in the SML could enhanced the dissolution processes and the diffusive transfer between SML and surface sea water. They estimated that the residence times ranged from 23 min. for pFe to 3.5 h for pCo in the SML after rain at FAST. From these timescales, the contribution of dissolution then diffusive process of dCo and dFe from SML to ML in the post-depositional dissolution processes could be considered. The increase of dissolved stocks suggested also that in the first hours after rain the dissolution processes were predominant on removal processes in the behaviour of dCo and dFe. Co and Fe being known to limit phytoplankton biomass, a biological uptake could be predominant if marine biota was limited for these elements. This was probably not the case here. The behaviour of Zn is more complicated to interpret since no enrichment was observed whereas the atmospheric dZn inputs represented around

12% of marine stocks. This unexpected behaviour could be explained by the predominant role of removal processes relative to post-depositional dissolution. The high solubility of Zn in Rain FAST (~86%), relative to solubility values of Fe (8%) or Co (52%), suggests that all the soluble Zn was already dissolved in the rain inputs before contacting with seawater.

~~We cannot exclude the possibility of lateral transport of metals from surrounding waters being enriched by the rain events of June 3 for example, as revealed by the increase in the 0–20 m Fe and Al inventories (Bressac et al., 2021). Another hypothesis to explain that higher stock increases of metals in the ML than the one derived from atmospheric deposition is related to post-deposition processes. Indeed, once deposited, the atmospheric particulate fraction could still be partly solubilized in seawater, as the solubilisation of TMs (e.g. Fe) could occur over several hours or days (Wagener et al., 2008; Wuttig et al., 2013; Desboeufs et al., 2014). This could lead to an underestimate of dissolved TMs atmospheric inputs. Moreover, the time lag between the rain and the first SML sampling (1 day) does not allow us to conclude on the role played by SML as a “trap” of the added dissolved metals by rain. However, results showed clearly the increase of dissolved TMs in the SML even 24 h after the rain (Fig. 9). Even if this increase could be due to dissolution processes (Tovar Sanchez et al., 2020), we cannot exclude that the residence time of dissolved atmospheric TMs in the SML was sufficient to mask the atmospheric inputs in the ML05+4 sample. It is also known that dissolved concentrations in the ML are subject to various biological processes such as phytoplankton uptake (Morel et al., 2003). The comparison between ML05+4 and ML05+12 samples performed after the rain shows that the dissolved and particulate stocks decreased quickly for all the TMs (not shown), in agreement with the predominance of removal processes (sedimentation, biological transfer, adsorption) on these stocks. However, the rate of decrease depended on the TMs, showing that some removal processes predominate over others depending on the metal. For example, the dissolved metals decrease could correspond to scavenging onto particles, which is a common physical-chemical process occurring in the ocean for Fe (Wagener et al., 2010; Bressac and Guieu., 2013) or Co (Migon et al., 2020). Finally, our results show that dust wet deposition was a net source of all the studied trace metals for SML both in the dissolved and particulate fraction. For ML, that the studied atmospheric dust inputs event werewas also a net source of particulate TMs Fe, Mn, and Zn, and dissolved Cu, Fe, Pb and Zn and Co for ML at FAST. Even if the wet deposition delivered TMs already as soluble forms (Fig. 8), our results showed that the wet deposition constitutes only a source of some of dissolved TMs for surface waters. Due to various marine post-deposition processes, it iwas more complicated to observe the effect of wet deposition on dissolved stocks, explaining why the SML and ML particulate stocks were more~~

931 impacted by rain than the dissolved stocks. The post-deposition dissolution of particulate rain inputs
932 could represent an additional pathway of dissolved TMs supply for the surface ocean, notably for
933 low soluble TMs in wet deposition. Thus, the dissolved atmospheric inputs could be underestimate
934 from the only measurements of atmospheric fluxes. On a timescale of hours, the Fe inventory was
935 the most impacted by the dusty rain input, both in dissolved and particulate phases, confirming that
936 the dust-rich rains are an net-external source of Fe to the surface Mediterranean Sea (Bonnet and
937 Guieu, 2006, Bressac et al., 2021).

939 4.2.3. Comparison between TMs wet atmospheric inputs and marine stocks in at the scale of the 940 western and central Mediterranean Sea

942 As ~~observed-discussed~~ from dissolved TMs stocks ~~at FAST-measured before and after the rains,~~
943 high surface marine TMs stocks station masked any additional input for several TMs a large part of
944 ~~uncertainties in the data analysis results from various removal processes of TMs after wet~~
945 ~~deposition, which could have time resolution shorter than the sampling step. In order to limit the~~
946 ~~effect on these potential processes in data analysis, he.~~ However, the collected rains (FAST and
947 ION) were originating from large rain systems covering more than 50 000 km² around the sampling
948 zone and were typical of Mediterranean wet deposition. The wet deposition could have so occurred
949 in any of the explored areas during the cruise. Here we further study the role of wet deposition by
950 comparing atmospheric dissolved fluxes to marine dissolved stocks ~~by using from~~ TMs profiles in
951 the ML at all 13 marine stations, i.e. 22 ML samplings, throughout the whole cruise (Fig. 10).
952 ~~Indeed, considering that the collected rains were originating from large rain systems covering more~~
953 ~~than 50 000 km² around the sampling zone and were typical of Mediterranean wet deposition, we~~
954 ~~hypothesized that they could have occurred in any of the explored areas during the cruise.~~
955 Exceptional intense dust deposition events have been recorded in the Mediterranean, reaching 20 g
956 m⁻² (Bonnet ~~et al and~~ Guieu, 2006). Sporadic and intense wet dust deposition higher than 1 g m⁻²
957 are regularly observed in the spring in the western Mediterranean basin (e.g., Vincent et al., 2016).
958 At the beginning of the cruise, an intense wet dust deposition event (not collected) occurred over
959 the South of Sardinia and over the Tyrrhenian Sea with fluxes reaching about 9 g m⁻² (Bressac et
960 al., 2021). In order to take into account the effect of such intense an event, we also estimated the
961 atmospheric fluxes of dissolved ~~metals-TMs~~ based on a 9 g m⁻² wet dust deposition event
962 considering using solubility values estimate found from in the Rain FAST (Fig. 10). Fe, Mn and Pb

solubility decreases with increasing dust load in Mediterranean rain samples (Theodosi et al., 2010), suggesting that this estimation is probably a maximum flux for such deposition event. However, recent studies from aerosol collected in Atlantic Ocean showed that Co and Mn solubility was little affected by dust load at the difference of Fe (Baker et al., 2020). The metal solubility decreasing with increasing dust load (Theodosi et al., 2010), this estimation constitutes probably a maximum value of the dissolved inputs of trace metals by such a dust deposition event. In addition to removal processes, the impact of rain inputs on TMs marine stocks is also controlled by MLD fluctuations which that we ignored in this work described above by using a fixed ML depth for the FAST and ION stations. However, As the variability of this MLD (7-21 m during the cruise, typical of Med thermal stratified period) could change the marine budgets by a factor of 3, we considered the measured MLD (Van Wambeke et al., 2020) at each station for calculating the TM marine stocks marine budgets of TMs at each station.

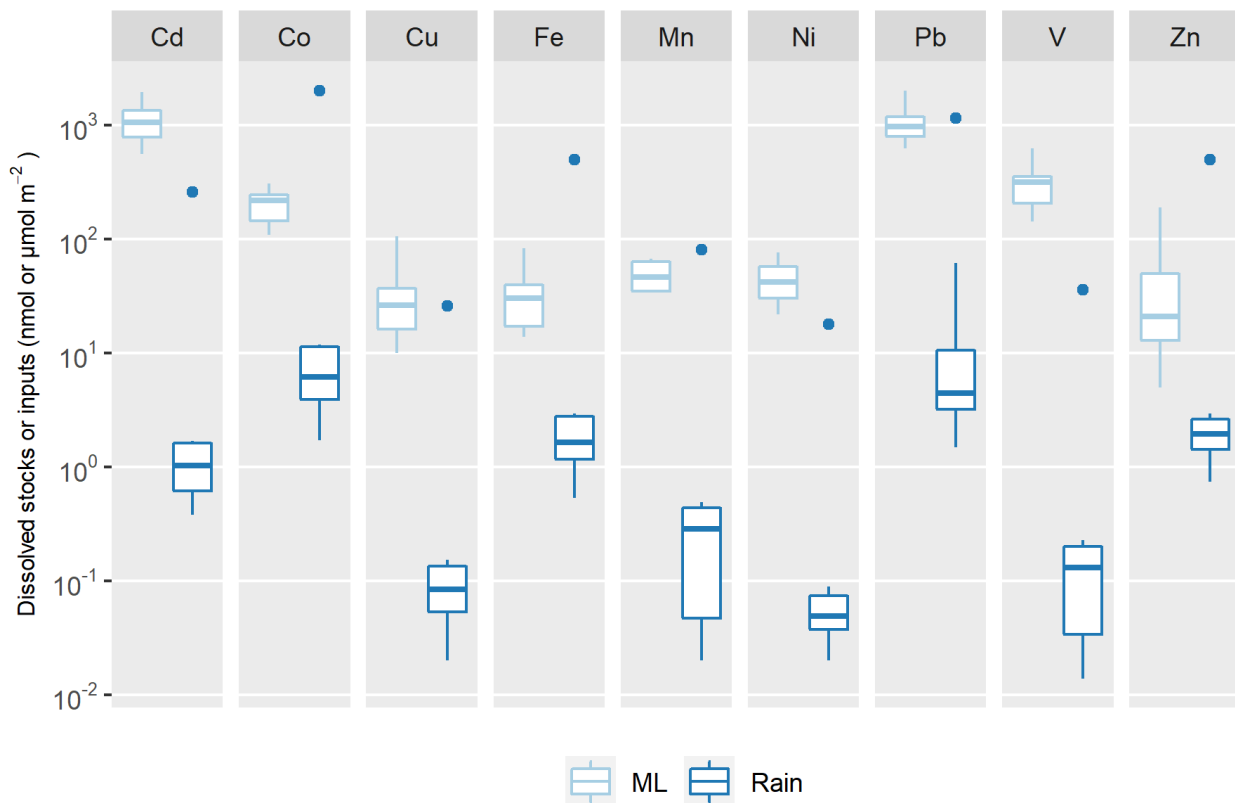


Figure 10: Comparison of marine stocks in the ML at all the stations occupied during the PEACETIME cruise (light blue boxes) with atmospheric inputs-deposition fluxes estimated (1) from ION and FAST rains (dark blue boxes) and (2) from an intense wet dust deposition event of 9 g m^{-2} (blue dots). Cd, Co and Pb stocks and fluxes are in nmol m^{-2} , and the other TMs in $\mu\text{mol m}^{-2}$. For Mn, marine stocks are derived from surface concentrations close to Corsica coasts (Wuttig et al., 2013:

samples OUT at 0, 5 and 10 m) and in the Ionian Sea (Saager et al., 1993: Bannock basin at 0, 10, and 15 m), as no measurement is available from the PEACETIME cruise. Boxes and whiskers as in Fig. 4.

Applying to the whole transect, the atmospheric inputs, obtained from our rain composition, were at least 100-fold smaller than the dissolved stocks in the mixed layer, except for Co, Fe and Zn. The atmospheric inputs represented more than 30% of the dissolved Zn stocks and 10 to 18% for Fe. For Co, the maximum atmospheric fluxes estimated during the cruise represented 5% of stocks. This significant input of dissolved Fe and dCo is in agreement with our field observations in the FAST ML. Here the comparison is based only on dissolved TMs in rain water, yet as discussed previously, the solubilisation-post-deposition deposition of atmospheric particles in the water column could further enrich the marine dissolved stocks for low soluble TMs, as Co, Fe, Mn, Ni, Pb or Ti. In the case of the intense dust deposition event, the dissolved inputs are of the same order of magnitude as marine stocks for Co, Fe, Mn, Pb and Zn. The enrichment in dissolved Fe and dMn was previously observed by Wuttig et al. (2013) after artificial dust seeding in large mesocosms (simulating a wet deposition event of 10 g m^{-2}). The surface seawater could be significantly affected by the deposition of these dissolved elements in the case of wet dust deposition. The marine TMs concentrations measured during the cruise being were typical of Mediterranean surface seawater concentrations, we can conclude from these comparisons that wet deposition events, notably wet dust deposition events, prove to be were an external source supply of dissolved Fe, Co and Zn for the Med Sea, and more generally for all TMs in case of intense wet dust deposition, TMs for the Mediterranean Sea during the period of thermal stratification.

5. Conclusions

This study provides both the dynamical properties and chemical characterization of two rain events waters collected in the open Mediterranean Sea, concurrently with TMs marine stocks in surface seawater. Our results are the only recent report of TM concentrations, EFs and fractional solubility values for TMs in rain samples collected in the remote Med Sea. By highlighting the discrepancy between TMs concentrations with the previous offshore and coastal rain studies, this work demonstrates the need to provide a new and recent database on metal-TM composition in Mediterranean rains in order to estimate the role of atmospheric TMs deposition. We have showed the representativeness of Rain FAST as typical of Saharan dust wet deposition as well in its chemical composition as well in its magnitude and extent, whereas Rain ION is a more typical of an low-perturbed anthropogenic background rain of for the remote Med Sea. On this basis, we suggest to use using the chemical composition of PEACETIME rains as a new reference for the

studies of TMs on wet deposition in the Med Sea. This study was focused on wet deposition, yet dry deposition is also an important source of TMs to surface waters in Med Sea. As the wet deposition fluxes decreased since the 90's due to mitigation, it is highly probable that the dry deposition fluxes were also changed. Further measurements of dry deposition in open Med Sea are needed in order to estimate its contribution in TM atmospheric inputs.

Since atmospheric TMs have been identified as critical oligo-nutrients for the marine biosphere, it is important to study the response of the receiving waters to atmospheric inputs. ~~our~~ This study is the first to provide *in situ* evidence that atmospheric wet deposition constitutes a significant external source for some of these elements to surface stratified Mediterranean seawater. ~~Our results show~~ We recommend that the original approach developed here is ~~very relevant in this purpose and could be~~ used in other parts of the world where atmospheric wet deposition is ~~suspected~~ thought to impact the marine biosphere, such as in HNLC areas.

Data availability. Guieu et al., Biogeochemical dataset collected during the PEACETIME cruise. SEANOE. <https://doi.org/10.17882/75747> (2020). Atmospheric Data are accessible on <http://www.obs-vlfr.fr/proof/php/PEACETIME/peacetime.php>.

Author contributions. KD and FF designed the study and wrote the manuscript; FF, ST, JFD, Ch.G made the on-board atmospheric measurements and sampling during the cruise; FF, ST and JD analysed the rain samples; MB, ATS, and ARR made the marine TMs sampling and analyses; PF was the reference scientist of PEGASUS, AF and FM managed all the technical preparation of atmospheric samplings, PC analysed the lidar data; KD, FD and Ce.G designed the cruise strategy; KD and Ce.G coordinated the PEACETIME project, FD coordinated the ChArMEx funding request, and near-real time and forecast survey of atmospheric conditions during the cruise; all the authors commented on the manuscript and contributed to its improvement.

Competing interests. The authors declare that they have no conflict of interest.

Special issue statement. This article is part of the special issue “Atmospheric deposition in the low-nutrient–low-chlorophyll (LNLC) ocean: effects on marine life today and in the future (ACP/BG inter- journal SI)”. It is not associated with a conference.

Acknowledgements. The authors wish to thank Thierry Alix the captain of the R/V *Pourquoi Pas ?* as well as the whole crew and technical staff for their involvement in the scientific operation. We gratefully thank Thibaut Wagener for his involvement in the trace-metals clean marine sampling and Mickaël Tharaud for

the HR-ICP-MS analysis. We thank the Leosphere Technical support team and especially Alexandre Menard for their remote assistance with LIDAR repair under difficult off-shore conditions. Hélène Ferré and the AERIS/SEDOO service are acknowledged for real-time collection during the cruise of maps from operational satellites and forecast models used in this study, with appreciated contributions of EUMETSAT and AERIS/ICARE for MSG/SEVIRI products. EUMETNET is acknowledged for providing the pan-European weather radar composite images through its OPERA programme. We acknowledge the US National Oceanic and Atmospheric Administration (NOAA) Air Resources Laboratory (ARL) for the provision of the HYSPLIT (HYbrid Single-Particle Lagrangian Integrated Trajectory) model via NOAA ARL READY website (<http://ready.arl.noaa.gov>) used in this publication. This study is a contribution to the PEACETIME project (<http://peacetime-project.org>; last accessed 05/04/2021), a joint initiative of the MERMEX and ChArMEx programmes supported by CNRS-INSU, IFREMER, CEA and Météo-France as part of the decadal meta-programme MISTRALS coordinated by CNRS-INSU. PEACETIME was endorsed as a process study by GEOTRACES and is also a contribution to IMBER and SOLAS international programs. The authors gratefully thank Rachel Shelley and the anonymous reviewer for their useful comments and critiques which have contributed to improve the manuscript.

References

- Achterberg, E. P., Braungardt, C. B., Sandford, R. C. and Worsfold, P. J.: UV digestion of seawater samples prior to the determination of copper using flow injection with chemiluminescence detection, *Anal. Chim. Acta*, 440, 27–36, [https://doi.org/10.1016/S0003-2670\(01\)00824-8](https://doi.org/10.1016/S0003-2670(01)00824-8), 2001.
- Al-Momani, I. F., Aygun, S., and Tuncel, G.: Wet Deposition of Major Ions and TMs in the Eastern Mediterranean Basin, *J. Geophys. Res. (Atmos.)*, 103, 8287–8299, <https://doi.org/10.1029/97JD03130>, 1998.
- Amato, F., Alastuey, A., Karanasiou, A., Lucarelli, F., Nava, S., Calzolari, G., Severi, M., Becagli, S., Gianelle, V. L., Colombi, C., Alves, C., Custódio, D., Nunes, T., Cerqueira, M., Pio, C., Eleftheriadis, K., Diapouli, E., Reche, C., Minguillón, M. C., Manousakas, M.-I., Maggos, T., Vratolis, S., Harrison, R. M., and Querol, X.: AIRUSE-LIFE+: a harmonized PM speciation and source apportionment in five southern European cities, *Atmos. Chem. Phys.*, 16, 3289–3309, <https://doi.org/10.5194/acp-16-3289-2016>, 2016.
- Annett, A. L., Lapi, S., Ruth, T. J., and Maldonado, M. T.: The effects of Cu and Fe availability on the growth and Cu:C ratios of marine diatoms, *Limnol. Oceanogr.*, 53, 2451–2461, <https://doi.org/10.4319/lo.2008.53.6.2451>, 2008.
- Avila, A., Queralt - Mitjans, I., and Alarcón, M.: Mineralogical composition of African dust delivered by red rains over northeastern Spain, *J. Geophys. Res. Atmos.*, 102, 21977–21996, <https://doi.org/10.1029/97JD00485>, 1997.
- Bacconnais, I., Rouxel, O., Dulaquais, G., and Boye, M.: Determination of the copper isotope composition of seawater revisited: A case study from the Mediterranean Sea, *Chem. Geol.*, 511, 465–480, <https://doi.org/10.1016/j.chemgeo.2018.09.009>, 2019.
- Baker, A. R., Adams, C., Bell, T. G., Jickells, T. D., and Ganzeveld, L., Estimation of atmospheric nutrient inputs to the Atlantic Ocean from 50°N to 50°S based on large-scale field sampling: Iron and other dust-associated elements, *Global Biogeochem. Cycles*, 27, 755– 767, doi:10.1002/gbc.20062, 2013.
- Baker, A. R., Li, M., & Chance, R., Trace metal fractional solubility in size-segregated aerosols from the tropical eastern Atlantic Ocean. *Global Biogeochemical Cycles*, 34, e2019GB006510. <https://doi.org/10.1029/2019GB006510>, 2020.
- Baker, A. R., and Jickells, T. D.: Atmospheric deposition of soluble trace elements along the Atlantic Meridional Transect (AMT), *Prog. Oceanogr.*, 158, 41– 51, <https://doi.org/10.1016/j.pocan.2016.10.002>, 2017.

1086 Becagli, S., Anello, F., Bommarito, C., Cassola, F., Calzolari, G., Iorio, T. D., Sarra, A. D., Gómez-Amo, J. L., Lucarelli,
1087 F., Marconi, M., and Meloni, D.: Constraining the ship contribution to the aerosol of the central Mediterranean, *Atmosp.*
1088 *Chem. Phys.*, 17, 2067–2084, <https://doi.org/10.5194/acp-17-2067-2017>, 2017.

1089 Bergametti, G., Gomes, L., Remoudaki, E., Desbois, M., Martin, D., and Buat-Ménard, P.: Present transport and
1090 deposition patterns of African dusts to the North-Western Mediterranean, in *Paleoclimatology and Paleometeorology:*
1091 *Modern and past patterns of global atmospheric transport*, Leinen, M., and Sarnthein, M., Eds., Springer, Dordrecht,
1092 NATO ASI Ser. C, 282, 227–252, https://doi.org/10.1007/978-94-009-0995-3_9, 1989.

1093 Béthoux, J.P., Courau, P., Nicolas, E., and Ruiz-Pino, D.: Trace metal pollution in the Mediterranean Sea, *Oceanol.*
1094 *Acta* 13, 481–488, <https://archimer.ifremer.fr/doc/00103/21418/> (last accessed 03 July 2021), 1990.

1095 Bonnet, S. and Guieu, C.: Dissolution of atmospheric iron in seawater, *Geophys. Res. Lett.*, 31, L03303,
1096 <https://doi.org/10.1029/2003GL018423>, 2004.

1097 Bonnet, S., and Guieu, C.: Atmospheric forcing on the annual iron cycle in the western Mediterranean Sea: A 1-year
1098 survey, *J. Geophys. Res.*, 111, C09010, <https://doi.org/10.1029/2005JC003213>, 2006.

1099 Bove, M. C., Brotto, P., Calzolari, G., Cassola, F., Cavalli, F., Fermo, P., Hjorth, J., Massabò, D., Nava, S., Piazzalunga,
1100 A., and Schembari, C.: PM₁₀ source apportionment applying PMF and chemical tracer analysis to ship-borne
1101 measurements in the Western Mediterranean, *Atmos. Environ.*, 125, 140–151,
1102 <https://doi.org/10.1016/j.atmosenv.2015.11.009>, 2016.

1103 Bressac, M., and Guieu, C.: Post-depositional processes: What really happens to new atmospheric iron in the ocean's
1104 surface?, *Global Biogeochem. Cycles*, 27, 859– 870, doi:[10.1002/gbc.20076](https://doi.org/10.1002/gbc.20076), 2013

1105 ~~Bressac, M., Wagener, T., Leblond, N., Tovar-Sánchez, A., Ridame, C., Taillandier, V., Albani, S., Guasco, S., Dufour,~~
1106 ~~A., Jacquet, S. H. M., Dulac, F., Desboeufs, K., and Guieu, C.: Subsurface iron accumulation and rapid aluminum~~
1107 ~~removal in the Mediterranean following African dust deposition, *Biogeosciences*, 18, 6435–6453,~~
1108 ~~<https://doi.org/10.5194/bg-18-6435-2021>, 2021~~~~Bressac, M., Wagener, T., Leblond, N., Tovar-Sánchez, A., Ridame, C.,~~
1109 ~~Albani, S., Guasco, S., Dufour, A., Jacquet, S., Dulac, F., Desboeufs, K., and Guieu, C.: Subsurface iron accumulation~~
1110 ~~and rapid aluminium removal in the Mediterranean following African dust deposition, *Biogeosciences Discuss.*,~~
1111 ~~<https://doi.org/10.5194/bg-2021-87>, in review, 2021.~~

1112 Bruland, K. W., Franks, R. P., Knauer, G. A. and Martin, J. H.: Sampling and analytical methods for the determination
1113 of copper, cadmium, zinc, and nickel at the nanogram per liter level in sea water, *Anal. Chim. Acta*, 105, 233–245,
1114 [https://doi.org/10.1016/S0003-2670\(01\)83754-5](https://doi.org/10.1016/S0003-2670(01)83754-5), 1979.

1115 Buat-Ménard, P., and Chesselet, R.: Variable influence of the atmospheric flux on the trace metal chemistry of oceanic
1116 suspended matter, *Earth Planet. Sci. Lett.*, 42, 399–411, [https://doi.org/10.1016/0012-821X\(79\)90049-9](https://doi.org/10.1016/0012-821X(79)90049-9), 1979.

1117 Buat-Ménard, P.: Particle geochemistry in the atmosphere and oceans, In: *Air-Sea Exchange of Gases and Particles*,
1118 Liss P.S., Slinn W.G.N. Editors, NATO ASI Series C, 108, 455–532, Springer, Dordrecht, [https://doi.org/10.1007/978-](https://doi.org/10.1007/978-94-009-7169-1_8)
1119 [94-009-7169-1_8](https://doi.org/10.1007/978-94-009-7169-1_8), 1983..

1120 Chance, R., Jickells, T. D. and Baker, A.R.: Atmospheric Trace Metal Concentrations, Solubility and Deposition Fluxes
1121 in Remote Marine Air over the South-East Atlantic, *Mar. Chem.*, 177, 45–56,
1122 <https://doi.org/10.1016/j.marchem.2015.06.028>, 2015.

1123 Chazette, P., Flamant, C., Totems, J., Gaetani, M., Smith, G., Baron, A., Landsheere, X., Desboeufs, K., Doussin, J.-
1124 F., and Formenti, P.: Evidence of the complexity of aerosol transport in the lower troposphere on the Namibian coast
1125 during AEROCLO-sA, *Atmos. Chem. Phys.*, 19, 14979–15005, <https://doi.org/10.5194/acp-19-14979-2019>, 2019.

1126 Chazette, P., Totems, J., Ancellet, G., Pelon, J., and Sicard, M.: Temporal consistency of lidar observations during
1127 aerosol transport events in the framework of the ChArMEx/ADRIMED campaign at Minorca in June 2013, *Atmos.*
1128 *Chem. Phys.*, 16, 2863–2875, <https://doi.org/10.5194/acp-16-2863-2016>, 2016.

1129 Chester, R., Nimmo, M., Corcoran, P. A.: Rain water-aerosol trace metal relationships at Cap Ferrat: a coastal site in
1130 the Western Mediterranean, *Mar. Chem.*, 58, 293–312, [https://doi.org/10.1016/S0304-4203\(97\)00056-X](https://doi.org/10.1016/S0304-4203(97)00056-X), 1997.

1131 Desboeufs, K., Losno, R., Vimeux, F., Cholbi, S.: the pH-dependent dissolution of wind transported Saharan dust. *J.*
1132 *Geophys. Res.*, 104, 21287–21299, <https://doi.org/10.1029/1999JD900236>, 1999.

1133 [Desboeufs, K. V., Sofikitis, A., Losno, R., Colin, J. L., and Ausset, P.: Dissolution and solubility of trace metals from](#)
1134 [natural and anthropogenic aerosol particulate matter, *Chemosphere*, 58, 195–203,](#)
1135 <https://doi.org/10.1016/j.chemosphere.2004.02.025>, 2005.

1136 Desboeufs, K., Leblond, N., Wagener, T., Bon Nguyen, E., Guieu, C.: Chemical fate and settling of mineral dust in
1137 surface seawater after atmospheric deposition observed from dust seeding experiments in large mesocosms,
1138 *Biogeosciences*, 11, 5581–5594, <https://doi.org/10.5194/bg-11-5581-2014>, 2014.

1139 Desboeufs, K., Bon Nguyen, E., Chevaillier, S., Triquet, S., and Dulac, F.: Fluxes and sources of nutrient and trace
1140 metal atmospheric deposition in the northwestern Mediterranean, *Atmos. Chem. Phys.*, 18, 14477–14492,
1141 <https://doi.org/10.5194/acp-18-14477-2018>, 2018.

1142 Desboeufs, K.: Trace metals and contaminants deposition, in *Atmospheric Chemistry in the Mediterranean – Vol. 2,*
1143 *From Pollutant Sources to Impacts*, edited by Dulac, F., Sauvage, S., and Hamonou, E., Springer, Cham, Switzerland,
1144 in press, 2021.

1145 [Duce, R. A., P. S. Liss, J. T. Merrill, E. L. Atlas, P. Buat-Menard, B. B. Hicks, J. M. Miller, J. M. Prospero, R. Arimoto,](#)
1146 [T. M. Church, W. Ellis, J. N. Galloway, L. Hansen, T. D. Jickells, A. H. Knap, K. H. Reinhardt, B. Schneider, A.](#)
1147 [Soudine, J. J. Tokos, S. Tsunogai, R. Wollast, M. Zhou, *The atmospheric input of trace species to the world ocean,*](#)
1148 [Global Biogeochem. Cycles](#), 5(3), 193–259, doi:10.1029/91GB01778, 1991.

1149 Dulac, F.: Dynamique du transport et des retombées d’aérosols métalliques en Méditerranée occidentale, PhD
1150 Dissertation, Univ. Paris 7, 241 pp., 1986.

1151 [Dulaquais, G., H. Planquette, S. L’Helguen, M. J. A. Rijkenberg, and M. Boye, *The biogeochemistry of cobalt in the*](#)
1152 [Mediterranean Sea, *Global Biogeochem. Cycles*, 31, 377–399, doi:10.1002/2016GB005478, 2017.](#)

1153 Formenti, P., D’Anna, B., Flamant, C., Mallet, M., Piketh, S. J., Schepanski, K., Waquet, F., Auriol, F., Brogniez, G.,
1154 Burnet, F., Chaboureaud, J., Chauvigné, A., Chazette, P., Denjean, C., Desboeufs, K., Doussin, J., Elguindi, N.,
1155 Feuerstein, S., Gaetani, M., Giorio, C., Kopper, D., Mallet, M. D., Nabat, P., Monod, A., Solmon, F., Namwoonde, A.,
1156 Chikwililwa, C., Mushi, R., Welton, E. J., and Holben, B.: The Aerosols, Radiation and Clouds in southern Africa field
1157 campaign in Namibia: Overview, illustrative observations, and way forward, *Bull. Am. Meteorol. Soc.*, 100, 1277–1298,
1158 <https://doi.org/10.1175/BAMS-D-17-0278.1>, 2019.

1159 Frau, F., Caboi, R., and Cristini, A.: The impact of Saharan dust on TMs solubility in rainwater in Sardinia, Italy, In:
1160 *The Impact of Desert Dust Across the Mediterranean*, S. Guerzoni, and R. Chester (Eds.), Springer, Dordrecht, Environ.
1161 *Sci. Technol. Library*, 11, 285–290, https://doi.org/10.1007/978-94-017-3354-0_28, 1996.

1162 Fu, Y.F., Desboeufs, K., Vincent, J., Bon Nguyen, E., Laurent, B., Losno, R., and Dulac, F.: Estimating chemical
1163 composition of atmospheric deposition fluxes from mineral insoluble particles deposition collected in the western
1164 Mediterranean region, *Atmos. Meas. Tech.*, 10, 4389–4401, <https://doi.org/10.5194/amt-10-4389-2017>, 2017.

1165 Fu, F., Desboeufs, K., Triquet, S., Doussin J.-F., Giorio C., Chevaillier S., Feron A., Formenti, F., Maisonneuve F.,
1166 Riffautl, V.: Aerosol characterisation and quantification of trace element atmospheric dry deposition fluxes in remote
1167 Mediterranean Sea during PEACETIME cruise, *Atmos. Chem. Phys.*, in prep.

1168 Gallisai, R., Peters, F., Volpe, G., Basart., and Baldasano J. M.: Saharan Dust deposition may affect phytoplankton
1169 growth in the Mediterranean S. Sea at ecological time scales, *PLoS One*, 9, e110762,
1170 <https://doi.org/10.1371/journal.pone.0110762>, 2014.

1171 Guerzoni, S, E Molinaroli, P Rossini, G Rampazzo, G Quarantotto, S Cristini.: Role of desert aerosol in metal fluxes in
1172 the Mediterranean area, *Chemosphere*, 39, 229–246, [https://doi.org/10.1016/S0045-6535\(99\)00105-8](https://doi.org/10.1016/S0045-6535(99)00105-8), 1999b.

1173 Guieu, C., and Ridame, C., Impact of atmospheric deposition on marine chemistry and biogeochemistry, in:
1174 Atmospheric Chemistry in the Mediterranean - Vol. 2, From Air Pollutant Sources to Impacts, edited by Dulac, F.,
1175 Sauvage, S., and Hamonou, E., Springer, Cham, Switzerland, in press, 2021.

1176 Guieu, C., Chester, R., Nimmo, M., Martin, J. M., Guerzoni, S., Nicolas, E., Mateu, J., and Keyse, S.: Atmospheric
1177 input of dissolved and particulate metals to the North Western Mediterranean, *Deep Sea Res. II*, 44, 655–674,
1178 [https://doi.org/10.1016/S0967-0645\(97\)88508-6](https://doi.org/10.1016/S0967-0645(97)88508-6), 1997.

1179 Guieu, C., Loye-Pilot, M. D., Ridame, C., and Thomas, C.: Chemical Characterization of the Saharan dust endmember:
1180 Some biogeochemical implications for the Western Mediterranean Sea, *J. Geophys. Res.*, 107, 4258,
1181 <https://doi.org/10.1029/2001JD000582>, 2002.

1182 Guieu, C., Bonnet, S., Wagener, T., and Loÿe-Pilot, M.-D.: Biomass burning as a source of dissolved iron to the open
1183 ocean?, *Geophys. Res. Lett.*, 32, L19608, <https://doi.org/10.1029/2005GL022962>, 2005.

1184 Guieu, C, M.-D. Loÿe-Pilot, L. Benyahya, A. Dufour.: Spatial variability of atmospheric fluxes of metals (Al, Fe, Cd,
1185 Zn and Pb) and phosphorus over the whole Mediterranean from a one-year monitoring experiment: Biogeochemical
1186 implications, *Mar. Chem.*, 120, 164–178, <https://doi.org/10.1016/j.marchem.2009.02.004>, 2010.

1187 Guieu, C., D'Ortenzio, F., Dulac, F., Taillandier, V., Doglioli, A., Petrenko, A., Barrillon, S., Mallet, M., Nabat, P., and
1188 Desboeufs, K.: Introduction: Process studies at the air-sea interface after atmospheric deposition in the Mediterranean
1189 Sea – objectives and strategy of the PEACETIME oceanographic campaign (May–June 2017), *Biogeosciences*, 17,
1190 5563–5585, <https://doi.org/10.5194/bg-17-5563-2020>, 2020.

1191 Hardy, J. T.: The sea surface microlayer: biology, chemistry and anthropogenic enrichment, *Prog. Oceanogr.*, 11, 307–
1192 328, [https://doi.org/10.1016/0079-6611\(82\)90001-5](https://doi.org/10.1016/0079-6611(82)90001-5), 1982.

1193 Heimbürger, L. E., Migon, C., Dufour, A., Chiffolleau, J. F., and Cossa, D.: Trace metal concentrations in the North-
1194 western Mediterranean atmospheric aerosol between 1986 and 2008: Seasonal patterns and decadal trends, *Sci. Total*
1195 *Environ.*, 408, 2629–2638, <https://doi.org/10.1016/j.scitotenv.2010.02.042>, 2010.

1196 Heimbürger, A., Losno, R., Triquet, S., Dulac F., and Mahowald, N. M.: Direct measurements of atmospheric iron,
1197 cobalt and aluminium-derived dust deposition at Kerguelen Islands, *Global Biogeochem. Cycles*, 26, GB4016,
1198 <https://doi.org/10.1029/2012GB004301>, 2012.

1199 Heimbürger, A., Losno, R., and Triquet, S.: Solubility of iron and other trace elements in rainwater collected on the
1200 Kerguelen Islands (South Indian Ocean), *Biogeosciences*, 10, 6617–6628, <https://doi.org/10.5194/bg-10-6617-2013>,
1201 2013.

1202 Hersbach, H., Bell, B., Berrisford, P., Biavati, G., Horányi, A., Muñoz Sabater, J., Nicolas, J., Peubey, C., Radu, R.,
1203 Rozum, I., Schepers, D., Simmons, A., Soci, C., Dee, D., Thépaut, J-N.: ERA5 hourly data on single levels from 1979
1204 to present, Copernicus Climate Change Service (C3S) Climate Data Store (CDS),
1205 <https://doi.org/10.24381/cds.adbb2d47>, 2018.

1206 Herut, B., Krom, M. D., Pan, G., and Mortimer, R.: Atmospheric input of nitrogen and phosphorus to the Southeast
1207 Mediterranean: Sources, fluxes, and possible impact, *Limnol. Oceanogr.*, 44, 1683–1692,
1208 <https://doi.org/10.4319/lo.1999.44.7.1683>, 1999.

Hydes, D.J., and Liss, P.S.: Fluorimetric method for the determination of low concentrations of dissolved aluminium in natural waters, *Analyst*, 101, 922–931, 1976.

[GEOTRACES Intermediate Data Product Group, The GEOTRACES Intermediate Data Product 2021 \(IDP2021\). NERC EDS British Oceanographic Data Centre NOC. doi:10.5285/cf2d9ba9-d51d-3b7c-e053-8486abc0f5fd, 2021.](#)

Gonzalez, L., and Briottet, X.: North Africa and Saudi Arabia day/night sandstorm survey (NASCube). *Remote Sens.*, 9, 896, <https://doi.org/10.3390/rs9090896>, 2017.

Izquierdo, R., Benítez-Nelson, C. R., Masqué, P., Castillo, S., Alastuey, A., Castillo, S., Alastuey, A., and Avila, A.: Atmospheric phosphorus deposition in a near-coastal rural site in the NE Iberian Peninsula and its role in marine productivity, *Atmos. Environ.*, 49, 361–370, <https://doi.org/10.1016/j.atmosenv.2011.11.007>, 2012.

Izquierda-Rojano, S., García-Gomez, H., Aguilhaume, L., Santamaría, J. M., Tang, Y. S., Santamaría, C., Valiño, F., Lasheras, E., Alonso, R., Àvila, A., Cape, J. N., and Elustondo, D.: Throughfall and bulk deposition of dissolved organic nitrogen to holm oak forests in the Iberian Peninsula: flux estimation and identification of potential sources, *Environ. Pollut.*, 210, 104–112, <https://doi.org/10.1016/j.envpol.2015.12.002>, 2016.

[Jickells TD, Baker AR, Chance R., Atmospheric transport of trace elements and nutrients to the oceans. *Phil. Trans. R. Soc. A* 374: 20150286, <http://dx.doi.org/10.1098/rsta.2015.0286>, 2016](#)

Jordi, A., Basterretxea, G., Tovar-Sánchez, A., Alastuey, A. and Querol, X.: Copper aerosols inhibit phytoplankton growth in the Mediterranean Sea, *Proc. Nat. Acad. Sci.*, 109, 21246–21249, <https://doi.org/10.1073/pnas.1207567110>, 2012.

Kanakidou, M., Mihalopoulos, N., Kindap, T., Im, U., Vrekoussis, M., Gerasopoulos, E., Dermizaki, E., Unal, A., Koçak, M., Markakis, K., Melas, D., Kouvarakis, G., Youssef, A. F., Richter, A., Hatzianastassiou, N., Hilboll, A., Ebojie, F., Wittrock, F., von Savigny, C., Burrows, J. P., Ladstaetter-Weissenmayer, A., and Moubasher, H.: Megacities as hot spots of air pollution in the East Mediterranean, *Atmos. Environ.*, 45, 1223–1235, <https://doi.org/10.1016/j.atmosenv.2010.11.048>, 2011.

Kanellopoulou, E. A.: Determination of heavy metals in wet deposition of Athens, *Global NEST J.*, 3, 45–50, <https://doi.org/10.30955/gnj.000181>, 2001.

Longo, A. F., Ingall, E. D., Diaz, J. M., Oakes, M., King, L. E., Nenes, A., Mihalopoulos, N., Violaki, K., Avila, A., Benitez-Nelson, C. R., Brandes, J., McNulty, I., and Vine, D. J.: P-NEXFS analysis of aerosol phosphorus delivered to the Mediterranean Sea, *Geophys. Res. Lett.*, 41, 4043–4049, <https://doi.org/10.1002/2014GL060555>, 2014.

Losno, R.: Chimie d'éléments minéraux en traces dans les pluies méditerranéennes, Ph.D. thesis, Univ. Paris-Diderot de Paris 7, <https://tel.archives-ouvertes.fr/tel-00814327/document> (last accessed 4 July 2021), 1989.

Loje-Pilot, M.-D., and Martin, J. M.: Saharan dust input to the western Mediterranean: an eleven years record in Corsica, , In: *The Impact of Desert Dust Across the Mediterranean*, Guerzoni, S., Chester, R. (Eds.), Springer, Dordrecht, *Environ. Sci. Technol. Library*, 11, 191–199, https://doi.org/10.1007/978-94-017-3354-0_18, 1996.

Mackey, K. R. M., Buck, K. N., Casey, J. R., Cid, A., Lomas, M. W., Sohrin, Y., and Paytan, A.: Phytoplankton Responses to Atmospheric Metal Deposition in the Coastal and Open-Ocean Sargasso Sea, *Front. Microbiol.*, 3, 359, <https://doi.org/10.3389/fmicb.2012.00359>, 2012.

Mallet, M. D., D'Anna, B., Mème, A., Bove, M. C., Cassola, F., Pace, G., Desboeufs, K., Di Biagio, C., Doussin, J.-F., Maille, M., Massabò, D., Sciare, J., Zapf, P., di Sarra, A. G., and Formenti, P.: Summertime surface PM₁ aerosol composition and size by source region at the Lampedusa island in the central Mediterranean Sea, *Atmos. Chem. Phys.*, 19, 11123–11142, <https://doi.org/10.5194/acp-19-11123-2019>, 2019.

1249 Markaki, Z., Loëe-Pilot, M. D., Violaki, K., Benyahya, L., and Mihalopoulos, N.: Variability of atmospheric deposition
1250 of dis- solved nitrogen and phosphorus in the Mediterranean and possible link to the anomalous seawater N/P ratio,
1251 Mar. Chem., 120, 187–194, <https://doi.org/10.1016/j.marchem.2008.10.005>, 2010.

1252 Migon, C., Robin, T., Dufour, A., and Gentili, B.: Decrease of lead concentrations in the Western Mediterranean
1253 atmosphere during the last 20 years, Atmos. Environ., 42, 815–821, <https://doi.org/10.1016/j.atmosenv.2007.10.078>,
1254 2008.

1255 Migon, C., Heimbürger-Boavida, L.-E., Dufour, A., Chiffolleau, J.-F., and Cossa, D.: Temporal variability of dissolved
1256 trace metals at the DYFAMED time-series station, Northwestern Mediterranean, Mar. Chem., 225, 103846,
1257 <https://doi.org/10.1016/j.marchem.2020.103846>, 2020.

1258 [Millero, F.J., Chemical Oceanography \(4th ed.\). CRC Press. https://doi.org/10.1201/b14753, 2013.](https://doi.org/10.1201/b14753)

1259 Milne, A., Landing, W., Bizimis, M., and Morton, P.: Determination of Mn, Fe, Co, Ni, Cu, Zn, Cd and Pb in seawater
1260 using high resolution magnetic sector inductively coupled mass spectrometry (HR-ICP-MS), Analytica Chimica Acta,
1261 665, 200–207, <https://doi.org/10.1016/j.aca.2010.03.027>, 2010.

1262 Morel, F. M. M., Hudson, R. J. M., and Price, N. M: Limitation of productivity by trace metals in the sea, Limnol.
1263 Oceanogr, 36, 1742–1755, <https://doi.org/10.4319/lo.1991.36.8.1742>, 1991.

1264 Morel, F. M., Milligan, A. J., & Saito, M. A. Marine bioinorganic chemistry: the role of trace metals in the oceanic
1265 cycles of major nutrients. Treatise on geochemistry, 6, 625, <https://doi.org/10.1016/B0-08-043751-6/06108-9>, 2003.

1266 Morin, E., Krajewski, W. F., Goorich, D. C., Gao, X., and Sorooshian, S.: Estimating rainfall intensities from weather
1267 radar data: The scale-dependency problem, J. Hydrometeorol., 4, 782–797, [https://doi.org/10.1175/1525-7541\(2003\)004<0782:ERIFWR>2.0.CO;2](https://doi.org/10.1175/1525-7541(2003)004<0782:ERIFWR>2.0.CO;2), 2003.

1269 Morley, N. H., Burton, J. D., Tankere, S. P. C., and Martin, J.-M.: Distribution and behaviour of some dissolved trace
1270 metals in the western Mediterranean Sea, Deep Sea Res. II, 44, 675–691, [https://doi.org/10.1016/S0967-0645\(96\)00098-7](https://doi.org/10.1016/S0967-0645(96)00098-7), 1997.

1272 Nehir, M., and Koçak, M.: Atmospheric water-soluble organic nitrogen (WSON) in the eastern Mediterranean: origin
1273 and ramifications regarding marine productivity, Atmos. Chem. Phys., 18, 3603–3618, <https://doi.org/10.5194/acp-18-3603-2018>, 2018.

1275 Ochoa-Hueso, R., Allen, E. B., Branquinho, C., Cruz, C., Dias, T., Fenn, M. E., Manrique, E., Perez-Corona, M. E.,
1276 Sheppard, L. J., and Stock, W. D.: Nitrogen deposition effects on Mediterranean-type ecosystems: an ecological
1277 assessment, Environ. Pollut., 159, 2265–2279, <https://doi.org/10.1016/j.envpol.2010.12.019>, 2011.

1278 [OSPAR Commission: Atmospheric deposition of selected heavy metals and persistent organic pollutants to the OSPAR
1279 maritime area \(1990 – 2005\). Publication 375/2008, 2008.](https://doi.org/10.1016/j.marchem.2008.10.005)

1280 Özsoy, T., and Örnektekin, S.: TMs in Urban and Suburban Rainfall, Mersin, Northeastern Mediterranean, Atmos. Res.,
1281 94, 203–219, <https://doi.org/10.1016/j.atmosres.2009.05.017>, 2009.

1282 Pacyna, E. G., Pacyna, J. M., Fudala, J., Strzelecka-Jastrzab, E., Hlawiczka, S., Panasiuk, D., Nitter, S., Pregger, T.,
1283 Pfeiffer, H., and Friedrich, R.: Current and future emissions of selected heavy metals to the atmosphere from
1284 anthropogenic sources in Europe, Atmos. Environ., 41, 8557–8566, <https://doi.org/10.1016/j.atmosenv.2007.07.040>,
1285 2007.

1286 Paris, R., and Desboeufs, K. V.: Effect of atmospheric organic complexation on iron-bearing dust solubility, Atmos.
1287 Chem. Phys., 13, 4895–4905, <https://doi.org/10.5194/acp-13-4895-2013>, 2013.

1288 Pinedo-González, P., Joshua West, A., Tovar-Sánchez, A., Duarte, C. M., Marañón, E., Cermeño, P., González, N.,
1289 Sobrino, C., Huete-Ortega, M., Fernández, A., López-Sandoval, D. C., Vidal, M., Blasco, D., Estrada, M., and Sañudo-

1290 Wilhelmy, S. A.: Surface distribution of dissolved trace metals in the oligotrophic ocean and their influence on
1291 phytoplankton biomass and productivity, *Global. Biogeochem. Cycles*, 29, 1763–1781,
1292 <https://doi.org/10.1002/2015GB005149>, 2015.

1293 Powell, C. F., Baker, A. R., Jickells, T. D., Bange, H. W., Chance, R. J., and Yodanis, C.: Estimation of the atmospheric
1294 flux of nutrients and trace metals to the eastern tropical North Atlantic Ocean, *J. Atmos. Sci.*, 72, 4029–4045,
1295 <https://doi.org/10.1175/JAS-D-15-0011.1>, 2015.

1296 Pulido-Villena, E., Rérolle, V., and Guieu, C.: Transient fertilizing effect of dust in P-deficient LNLC surface ocean,
1297 *Geophys. Res. Lett.*, 37, L01603, <https://doi.org/10.1029/2009GL041415>, 2010.

1298 [Pulido-Villena, E., Desboeufs, K., Djaoudi, K., Van Wambeke, F., Barrillon, S., Doglioli, A., Petrenko, A., Taillandier,
1299 V., Fu, F., Gaillard, T., Guasco, S., Nunige, S., Triquet, S., and Guieu, C.: Phosphorus cycling in the upper waters of
1300 the Mediterranean Sea \(PEACETIME cruise\): relative contribution of external and internal sources, *Biogeosciences*,
1301 18, 5871–5889, <https://doi.org/10.5194/bg-18-5871-2021>, 2021.](#)

1302 Rahn, K. A.: The Chemical Composition of the Atmospheric Aerosol, Tech. Rept., Graduate School of Oceanography,
1303 Univ. Rhode Island, Kingston, RI, 265 pp., <https://books.google.fr/books?id=q-dOQAAMAAJ> (last accessed 04 July
1304 2021), 1976.

1305 Raut, J.-C., and Chazette, P.: Assessment of vertically-resolved PM10 from mobile lidar observations, *Atmos. Chem.*
1306 *Phys.*, 9, 8617–8638, <https://doi.org/10.5194/acp-9-8617-2009>, 2009.

1307 Richon, C., Dutay, J.-C., Dulac, F., Wang, R., and Balkanski, Y.: Modeling the biogeochemical impact of atmospheric
1308 phosphate deposition from desert dust and combustion sources to the Mediterranean Sea, *Biogeosciences*, 15, 2499–
1309 2524, <https://doi.org/10.5194/bg-15-2499-2018>, 2018a.

1310 Richon, C., Dutay, J.C., Dulac, F., Wang, R., Balkanski, Y., Nabat, P., Aumont, O., Desboeufs, K., Laurent, B., Guieu,
1311 C., and Raimbault, P.: Modeling the impacts of atmospheric deposition of nitrogen and desert dust-derived phosphorus
1312 on nutrients and biological budgets of the Mediterranean Sea, *Prog. Oceanogr.*, 163, 21–39,
1313 <https://doi.org/10.1016/j.pocean.2017.04.009>, 2018b.

1314 Ridame, C., Le Moal, M., Guieu, C., Ternon, E., Biegala, I. C., L’Helguen, S., and Pujo-Pay, M.: Nutrient control of
1315 N₂ fixation in the oligotrophic Mediterranean Sea and the impact of Saharan dust events, *Biogeosciences*, 8, 2773–
1316 2783, <https://doi.org/10.5194/bg-8-2773-2011>, 2011.

1317 Royer, P., Chazette, P., Lardier, M., and Sauvage, L.: Aerosol content survey by mini N₂-Raman lidar: Application to
1318 local and long-range transport aerosols, *Atmos. Environ.*, 45, 7487–7495,
1319 <https://doi.org/10.1016/j.atmosenv.2010.11.001>, 2011.

1320 Rudnick, R. L., and Gao, S.: Composition of the Continental Crust. In: *Treatise on Geochemistry*, Holland, H. D., and
1321 Turekian, K. K. (Editors), Elsevier, Amsterdam. 3, 1–64, 2003.

1322 Saager, P. M., Schijf, J., and de Baar, H. J. W.: Trace-metal distributions in seawater and anoxic brines in the eastern
1323 Mediterranean Sea, *Geochim. Cosmochim. Acta*, 57, 1419–1432, [https://doi.org/10.1016/0016-7037\(93\)90003-F](https://doi.org/10.1016/0016-7037(93)90003-F),
1324 1993.

1325 Sandroni, V., and Migon, C.: Atmospheric deposition of metallic pollutants over the Ligurian Sea: labile and residual
1326 inputs, *Chemosphere*, 47, 753–764, [https://doi.org/10.1016/s0045-6535\(01\)00337-x](https://doi.org/10.1016/s0045-6535(01)00337-x), 2002.

1327 Saltikoff, E., Haase, G., Delobbe, L., Gaussiat, N., Martet, M., Idziorek, D., Leijnse, H., Novák, P., Lukach, M., and
1328 Stephan, K.: OPERA the Radar Project, *Atmosphere*, 10, 320, <https://doi.org/10.3390/atmos10060320>, 2019.

1329 Sciare, J., Bardouki, H., Moulin, C., and Mihalopoulos, N.: Aerosol sources and their contribution to the chemical
1330 composition of aerosols in the Eastern Mediterranean Sea during summertime, *Atmos. Chem. Phys.*, 3, 291–302,
1331 <https://doi.org/10.5194/acp-3-291-2003>, 2003.

- Sedwick, P. N., Sholkovitz, E. R., and Church, T. M.: Impact of anthropogenic combustion emissions on the fractional solubility of aerosol iron: Evidence from the Sargasso Sea, *Geochem. Geophys. Geosyst.*, 8, Q10Q06, doi:10.1029/2007GC001586.
- Sherrell, R. M. and Boyle, E. A.: Zinc, chromium, vanadium and iron in the Mediterranean Sea, *Deep Sea Res. A*, 35, 1319–1334, [https://doi.org/10.1016/0198-0149\(88\)90085-4](https://doi.org/10.1016/0198-0149(88)90085-4), 1988.
- Smedley, P. L., and Kinniburgh, D. G.: Molybdenum in natural waters: A review of occurrence, distributions and controls, *Appl. Geochem.* 84, 387–432. <http://dx.doi.org/10.1016/j.apgeochem.2017.05.008>, 2017.
- Stortini, A. M., Cincinelli, A., Degli Innocenti, N., Tovar-Sánchez, A. and Knulst, J.: 1.12 - Surface Microlayer, In: *Comprehensive Sampling and Sample Preparation - Vol. 1: Sampling Theory and Methodology*, Pawliszyn, J. (Ed.-in-Chief), 223–246, Academic Press, Oxford, <https://doi.org/10.1016/B978-0-12-381373-2.00018-1>, 2012.
- Ternon, E., Guieu, C., Loÿe-Pilot, M. D., Leblond, N., Bosc, E., Gasser, B., Miquel, J. C., Martin, J.: The impact of Saharan dust on the particulate export in the water column of the North Western Mediterranean Sea, *Biogeosciences*, 7, 809–826, <https://doi.org/10.5194/bg-7-809-2010>, 2010.
- The Mermex Group, et al.: Marine ecosystems' responses to climatic and anthropogenic forcings in the Mediterranean, *Prog. Oceanogr.*, 91, 97–166, <https://doi.org/10.1016/j.pocean.2011.02.003>, 2011.
- Theodosi, C., Markaki, Z., Tselepides, A., and Mihalopoulos, N.: The significance of atmospheric inputs of soluble and particulate major and TMs to the Eastern Mediterranean Sea, *Mar. Chem.* 120, 154–163, <https://doi.org/10.1016/J.MARCHEM.2010.02.003>, 2010.
- Thieuleux, F., Moulin, C., Bréon, F. M., Maignan, F., Poitou, J., and Tanré, D.: Remote sensing of aerosols over the oceans using MSG/SEVIRI imagery, *Ann. Geophys.*, 23, 3561–3568, <https://doi.org/10.5194/angeo-23-3561-2005>, 2005.
- Tovar-Sánchez, A., Arrieta, J. M., Duarte, C. M., and Sañudo-Wilhelmy, S. A.: Spatial gradients in trace metal concentrations in the surface microlayer of the Mediterranean Sea, *Front. Mar. Sci.*, 1, 79, <https://doi.org/10.3389/fmars.2014.00079>, 2014.
- Tovar-Sánchez, A., González-Ortegón, E., and Duarte, C. M.: Trace metal partitioning in the top meter of the ocean, *Sci. Total Environ.*, 652, 907–914, <https://doi.org/10.1016/j.scitotenv.2018.10.315>, 2019.
- Tovar-Sánchez, A., Rodríguez-Romero, A., Engel, A., Zäncker, B., Fu, F., Marañón, E., Pérez-Lorenzo, M., Bressac, M., Wagener, T., Triquet, S., Siour, G., Desboeufs, K., and Guieu, C.: Characterizing the surface microlayer in the Mediterranean Sea: trace metal concentrations and microbial plankton abundance, *Biogeosciences*, 17, 2349–2364, <https://doi.org/10.5194/bg-17-2349-2020>, 2020.
- Travnikov, O., Ilyin I., O. Rozovskaya, M. Varygina, W. Aas, H. T. Uggerud, K. Mareckova, and R. Wankmueller, *Long-term Changes of Heavy Metal Transboundary Pollution of the Environment (1990-2010)*, EMEP Status Report 2/2012, 2012.
- Van Wambeke, F., Pulido, E., Catala, P., Dinasquet, J., Djaoudi, K., Engel, A., Garel, M., Guasco, S., Marie, B., Nunige, S., Taillandier, V., Zäncker, B., and Tamburini, C.: Spatial patterns of ectoenzymatic kinetics in relation to biogeochemical properties in the Mediterranean Sea and the concentration of the fluorogenic substrate used, *Biogeosciences*, 18, 2301–2323, <https://doi.org/10.5194/bg-18-2301-2021>, 2021a.
- Van Wambeke, F., Taillandier, V., Desboeufs, K., Pulido-Villena, E., Dinasquet, J., Engel, A., Marañón, E., Ridame, C., and Guieu, C.: Influence of atmospheric deposition on biogeochemical cycles in an oligotrophic ocean system, *Biogeosciences*, 18, 5699–5717, <https://doi.org/10.5194/bg-18-5699-2021>, 2021b. Van Wambeke, F., Taillandier, V., Desboeufs, K., Pulido-Villena, E., Dinasquet, J., Engel, A., Marañón, E., Ridame, C., and Guieu, C.: Influence of atmospheric deposition on biogeochemical cycles in an oligotrophic ocean system, *Biogeosciences Discuss.*, <https://doi.org/10.5194/bg-2020-411>, in review, 2020.

1375 Vincent, J., Laurent, B., Losno, R., Bon Nguyen, E., Rouillet, P., Sauvage, S., Chevaillier, S., Coddeville, P.,
1376 Ouboulmane, N., di Sarra, A. G., Tovar-Sánchez, A., Sferlazzo, D., Massanet, A., Triquet, S., Morales Baquero, R.,
1377 Fornier, M., Coursier, C., Desboeufs, K., Dulac, F., and Bergametti, G.: Variability of mineral dust deposition in the
1378 western Mediterranean basin and south-east of France, *Atmos. Chem. Phys.*, 16, 8749–8766,
1379 <https://doi.org/10.5194/acp-16-8749-2016>, 2016.

1380 Violaki, K., Bourrin, F., Aubert, D., Kouvarakis, G., Delsaut, N., and Mihalopoulos, N.: Organic phosphorus in
1381 atmospheric deposition over the Mediterranean Sea: An important missing piece of the phosphorus cycle, *Prog.*
1382 *Oceanogr.*, 163, 50–58, <https://doi.org/10.1016/j.pocean.2017.07.009>, 2018.

1383 Wagener, T., Pulido-Villena, E., and Guieu, C.: Dust iron dis-solution in seawater: Results from a one-year time-series
1384 in the Mediterranean Sea, *Geophys. Res. Lett.*, 35, L16601, <https://doi.org/10.1029/2008GL034581>, 2008.

1385 Wagener, T., Guieu, C., and Leblond, N.: Effects of dust deposition on iron cycle in the surface Mediterranean Sea:
1386 results from a mesocosm seeding experiment, *Biogeosciences*, 7, 3769–3781, <https://doi.org/10.5194/bg-7-3769-2010>,
1387 2010.

1388 [Weinzierl, B., Ansmann, A., Prospero, J. M., Althausen, D., Benker, N., Chouza, F., Dollner, M., Farrell, D., Fomba,](#)
1389 [W. K., Freudenthaler, V., Gasteiger, J., Groß, S., Haarig, M., Heinold, B., Kandler, K., Kristensen, T. B., Mayol-](#)
1390 [Bracero, O. L., Müller, T., Reitebuch, O., Sauer, D., Schäfler, A., Schepanski, K., Spanu, A., Tegen, I., Toledano, C.,](#)
1391 [& Walser, A.. The Saharan Aerosol Long-Range Transport and Aerosol–Cloud-Interaction Experiment: Overview and](#)
1392 [Selected Highlights, BAMS, 98\(7\), 1427-1451, https://doi.org/10.1175/BAMS-D-15-00142.1, 2017.](#)

1393 Wurl, O.: Practical Guidelines for the Analysis of Seawater, 1st ed., CRC Press., 2009.

1394 Wuttig, K., Wagener, T., Bressac, M., Dammshäuser, A., Streu, P., Guieu, C., and Croot, P. L.: Impacts of dust
1395 deposition on dissolved trace metal concentrations (Mn, Al and Fe) during a mesocosm experiment, *Biogeosciences*,
1396 10, 2583–2600, <https://doi.org/10.5194/bg-10-2583-2013>, 2013.

1397 Yoon, Y. Y., Martin, J.-M., and Cotté, M. H.: Dissolved trace metals in the western Mediterranean Sea: total
1398 concentration and fraction isolated by C18 Sep-Pak technique, *Mar. Chem.*, 66, 129–148,
1399 [https://doi.org/10.1016/S0304-4203\(99\)00033-X](https://doi.org/10.1016/S0304-4203(99)00033-X), 1999.

